Cell Reports

Article

Phosphoprotein dynamics of interacting T cells and tumor cells by HySic

Graphical abstract

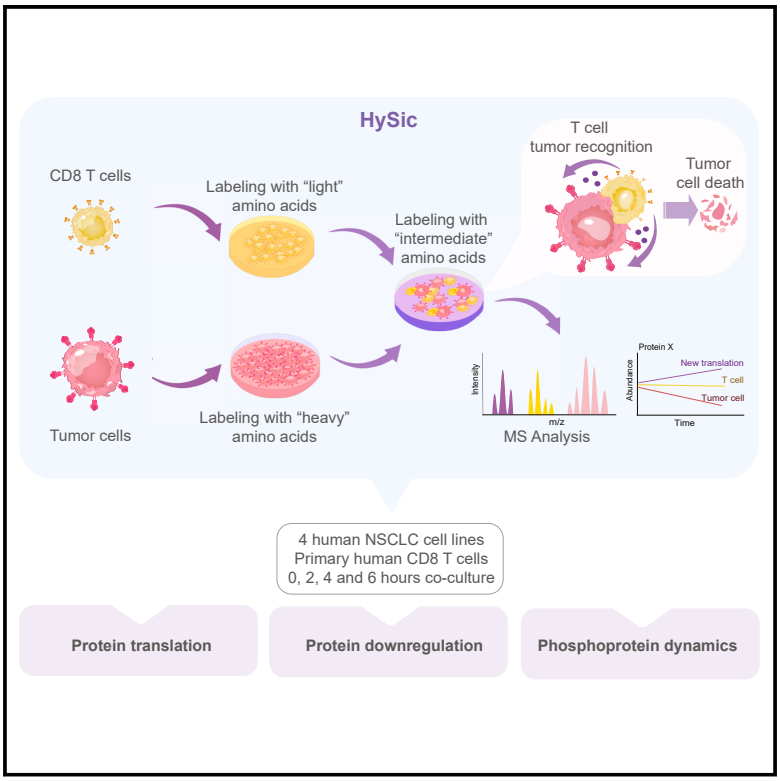

Highlights

- HySic is a method to study cell-specific phosphoprotein dynamics in interacting cells
- HySic quantifies protein translation, protein downregulation, and phosphoprotein signaling
- HySic of T cell:tumor cell interactions identifies RHO/RAC/PAK1 pathway as potential target
- PAK1 inhibition sensitizes cultured tumor cells to T cell killing

Authors

Sofía Ibáñez-Molero, Joannes T.M. Pruijs, Alisha Atmopawiro, ..., Maarten Altelaar, Daniel S. Peeper, Kelly E. Stecker

Correspondence

m.altelaar@nki.nl (M.A.),
d.peeper@nki.nl (D.S.P.)

In brief

Ibáñez-Molero et al. establish HySic, a method to quantify protein translation, downregulation and phosphorylation upon T cell:tumor cell interactions. Their study highlights both known and new proteins whose abundance and activity changes upon the interactions, some of which may be targeted to increase tumor susceptibility to T cell killing.

Ibáñez-Molero et al., 2024, Cell Reports *43*, 113598
January 23, 2024
https://doi.org/10.1016/j.celrep.2023.113598

Cell Reports

CellPress
OPEN ACCESS

Article

Phosphoprotein dynamics of interacting T cells and tumor cells by HySic

Sofía Ibáñez-Molero,[1,4] Joannes T.M. Pruijs,[1,4] Alisha Atmopawiro,[1] Fujia Wang,[2] Alexandra M. Terry,[1] Maarten Altelaar,[2,*] Daniel S. Peeper,[1,3,4,5,*] and Kelly E. Stecker[2]

[1]Division of Molecular Oncology and Immunology, Netherlands Cancer Institute, Plesmanlaan 121, 1066 CX Amsterdam, the Netherlands
[2]Biomolecular Mass Spectrometry and Proteomics, Center for Biomolecular Research and Utrecht Institute for Pharmaceutical Sciences, Utrecht University, Padualaan 8, 3584 CH Utrecht, the Netherlands
[3]Department of Pathology, VU University Amsterdam, 1081 HV Amsterdam, the Netherlands
[4]Oncode Institute, 3521 AL Utrecht, the Netherlands
[5]Lead contact
*Correspondence: m.altelaar@nki.nl (M.A.), d.peeper@nki.nl (D.S.P.)
https://doi.org/10.1016/j.celrep.2023.113598

SUMMARY

Functional interactions between cytotoxic T cells and tumor cells are central to anti-cancer immunity. However, our understanding of the proteins involved is limited. Here, we present HySic (hybrid quantification of stable isotope labeling by amino acids in cell culture [SILAC]-labeled interacting cells) as a method to quantify protein and phosphorylation dynamics between and within physically interacting cells. Using co-cultured T cells and tumor cells, we directly measure the proteome and phosphoproteome of engaged cells without the need for physical separation. We identify proteins whose abundance or activation status changes upon T cell:tumor cell interaction and validate our method with established signal transduction pathways including interferon γ (IFNγ) and tumor necrosis factor (TNF). Furthermore, we identify the RHO/RAC/PAK1 signaling pathway to be activated upon cell engagement and show that pharmacologic inhibition of PAK1 sensitizes tumor cells to T cell killing. Thus, HySic is a simple method to study rapid protein signaling dynamics in physically interacting cells that is easily extended to other biological systems.

INTRODUCTION

Immunotherapies, such as immune checkpoint blockade (ICB) therapy, have revolutionized cancer treatment. They act by targeting immune-suppressive protein interactions in the tumor microenvironment (TME). However, the majority of patients still fail to achieve a durable clinical benefit, due to therapy resistance, whether upfront or on therapy.[1–3] Cytotoxic T cells recognize tumor cells by T cell receptor (TCR)-antigen-major histocompatibility complex (MHC) class I interactions and subsequently trigger apoptosis. This inter-cellular communication serves as a critical event in the process of tumor eradication. Functional interrogation of T cell:tumor interactions using genetic approaches such as whole-genome CRISPR-Cas9 screens[4,5] has proven a successful strategy to identify genes vital to the defense of tumor cells against T cell attack. For example, we previously showed that perturbation of specific components of pro-survival tumor necrosis factor (TNF) signaling, like TRAF2 and RNF31, strongly sensitizes tumors to killing by CD8 T and natural killer (NK) cells, *in vitro* and *in vivo*.[6,7] Together, these functional studies revealed several tumor resistance mechanisms, including lack of antigen presentation and deficiencies in autophagy, interferon γ (IFNγ), and TNF pathways.[5,6] However, such genetic approaches cannot expose resistance mechanisms that rely on dynamic protein networks and signal transduction events that are driven by post-translation modifications (PTMs), such as phosphorylation. This makes our understanding of the functional interactions between T cells and tumor cells rather gene-centric and rudimentary.

Phosphoproteomics techniques have allowed the identification of drug resistance mechanisms in tumors[8] and mechanisms of T cell key signaling molecules like TCR and PD-1.[9,10] The phosphoproteome serves as a primary regulator of cell signaling during cell-cell interactions,[11] and in the last decade, accuracy in quantitative techniques has remarkably increased.[12,13] However, standard proteomic and phosphoproteomic approaches quantify digested proteins from homogenized lysates, in which the cellular context is lost during sample preparation. These methods, therefore, cannot distinguish the cellular origin of protein content and do not allow for cell-specific information to be extracted from a mixed cell system such as T cells engaged with tumor cells. The need to investigate communication between cytotoxic T cells and tumor cells, two distinct cell types that physically interact, thus presents a technical challenge for (phospho)proteomic studies: preservation of cell-type-specific information, which is what we address here.

One approach to solve the challenge of deciphering mixed proteomes derived from interacting cells is the use of stable isotope labeling by amino acids in cell culture (SILAC).[14,15] The proteome of different cells can be uniquely labeled by metabolic

incorporation of essential amino acids that contain stable isotopes, thus providing a unique mass signature for each cell type. Traditional SILAC applications use labeling strategies to distinguish different experimental conditions by mixing labeled proteomes just before or after cell lysis. The relative mass spectrometry (MS) intensity of the labeled peptides is then used to quantify protein and phosphopeptide changes. This standard method utilizes SILAC for sample multiplexing and quantification during MS analysis. In addition, a handful of studies have applied SILAC labeling to study mixed cell types interacting in co-culture.[16,17] However, those studies either did not examine both interacting cell types, or they required physical separation by fluorescence-activated cell sorting (FACS) after interaction, which can induce undesired changes in the phosphoproteome. Moreover, they utilize SILAC in the traditional way, as a ratio for quantification.

To overcome these technical limitations, here we developed a strategy in which SILAC labels are used as barcodes to distinguish the two interacting cell types in co-cultures. A concomitant second method of label-free quantification (LFQ) is applied to measure protein and phosphorylation dynamics for each SILAC signature separately. This hybrid-quantitative MS approach using both SILAC and LFQ allows for direct monitoring of both protein and phosphorylation dynamics over many different conditions, because one is not limited to a fixed set of ratios defined by SILAC. We termed this method hybrid quantification of SILAC-labeled interacting cells (HySic) to probe rapid proteome and phosphoproteome dynamics. To illustrate the utility of this method, we made use of a T cell:tumor cell co-culture system that we successfully used previously in genetic screens to identify genes critically involved in tumor sensitivity to T cells. Leveraging the standard SILAC labels, we deciphered three types of information in each experimental condition: protein degradation and phosphorylation occurring within T cells and within tumor cells, and the induction and phosphorylation of newly translated proteins upon co-culturing. After validating HySic findings from each of these categories using independent techniques, we explored T cell:tumor cell responses to uncover actionable targets. We further validated one target involved in both T cell and tumor cell phosphorylation responses. Altogether, we present the robustness and applicability of HySic as an easy platform to unravel protein dynamics and phosphorylation in functional (heterotypic) cell-cell interactions.

RESULTS

Developing HySic

To study the signaling dynamics of T cell:tumor interactions, we made use of a system we established previously for melanoma and non-small cell lung cancer (NSCLC).[18] In this model, we genetically engineered tumor cells to express the MHC class I (specifically HLA-A*02:01) protein capable of presenting the tumor antigen MART-1, as well as the MART-1 epitope itself. On the other hand, CD8 T cells were isolated from healthy donors and subsequently retrovirally transduced with a MART-1-specific TCR (1D3 TCR) (Figure 1A). Consistent with our previous results, we observed that upon co-culturing, T cells were able to recognize the tumor cells. We validated that upon tumor cell encounter, T cells became activated, as judged by the production of the cytotoxic molecules IFNγ and TNF (Figure 1B). This ultimately led to tumor cell-cycle arrest and/or cell death (Figure 1C). These results illustrate the specificity and utility of this T cell:tumor co-culture model, providing the foundation to develop a method to analyze the functional interactions in more depth.

We tested whether this co-culture system allows for the measurement of protein and phosphorylation changes upon T cell:tumor cell engagement. After 16 h, the T cell-containing supernatant was removed, followed by trypsinization of the fraction of tumor cells that were still conjugated to the T cells. This physical separation was performed in a panel of 15 human NSCLC cell lines, in which we observed that the purity of each cell fraction following separation was on average low: only 44% of the isolated T cell population was pure and did not contain tumor cells, and only 71% of the isolated tumor cells were free from T cell contamination (Figure S1A). This result indicates that there is a high percentage of contamination of the other cell type (whether T cells or tumor cells) in the separated fractions. This mixed cell content would complicate the interpretation of the proteomic and phosphoproteomic data by MS analysis. To circumvent this problem, we developed a SILAC-based labeling method for analyzing functional interactions in the T cell:tumor cell co-cultures, as this could identify proteins of different cell origin from two cell mixed proteomes based on their unique mass signatures.

We labeled T cells and tumor cells separately with "light" ($^{0}K^{0}R$) and "heavy" ($^{8}K^{10}R$) amino acids, respectively. After >93% label incorporation was confirmed for four tumor cell lines (Figure S1B), the two cell types were co-cultured for up to 6 h in medium containing "intermediate" ($^{4}K^{6}R$) amino acid isotopes. Cells from complete co-cultures were then pelleted, lysed, and analyzed by liquid chromatography (LC)-MS for proteome and phosphoproteome analyses. The incorporation of three different amino acid isotope labels allows for the potential identification of proteins from distinct origins: T cells ($^{0}K^{0}R$), tumor cells ($^{8}K^{10}R$), and newly synthesized proteins from either cell type ($^{4}K^{6}R$). We will refer to these isotopes as T cell-protein label, tumor-protein label, and newly synthesized-protein label, respectively. In this way, we exploited SILAC labels as barcodes to distinguish the two cell types. We next used a second MS quantification method, label-free quantification (LFQ), to measure the change in protein and phosphosite abundance for each SILAC label independently across samples (Figure 1D). Together, this constitutes a hybrid quantification approach to measure SILAC-labeled interacting cells (HySic). We applied HySic to analyze four different NSCLC cell lines in co-culture with T cells as a function of time (0, 2, 4, and 6 h) and at a 1:1 T cell:tumor cell ratio. The selected time points were before the onset of (substantial) tumor cell death (Figure S1C). We conducted these experiments in two independent batches. To control for background translation, we also incubated T cells and tumor cells independently in newly synthesized-protein-label media for 4 h.

We analyzed the total number of unique proteins and phosphosites quantified by HySic (Figures 1E, S1D, and S1E). In tumor cell fractions, we measured more proteins and phosphosites than in the T cell or newly synthesized fractions. This was likely due to a higher protein content in tumor cells owing to their

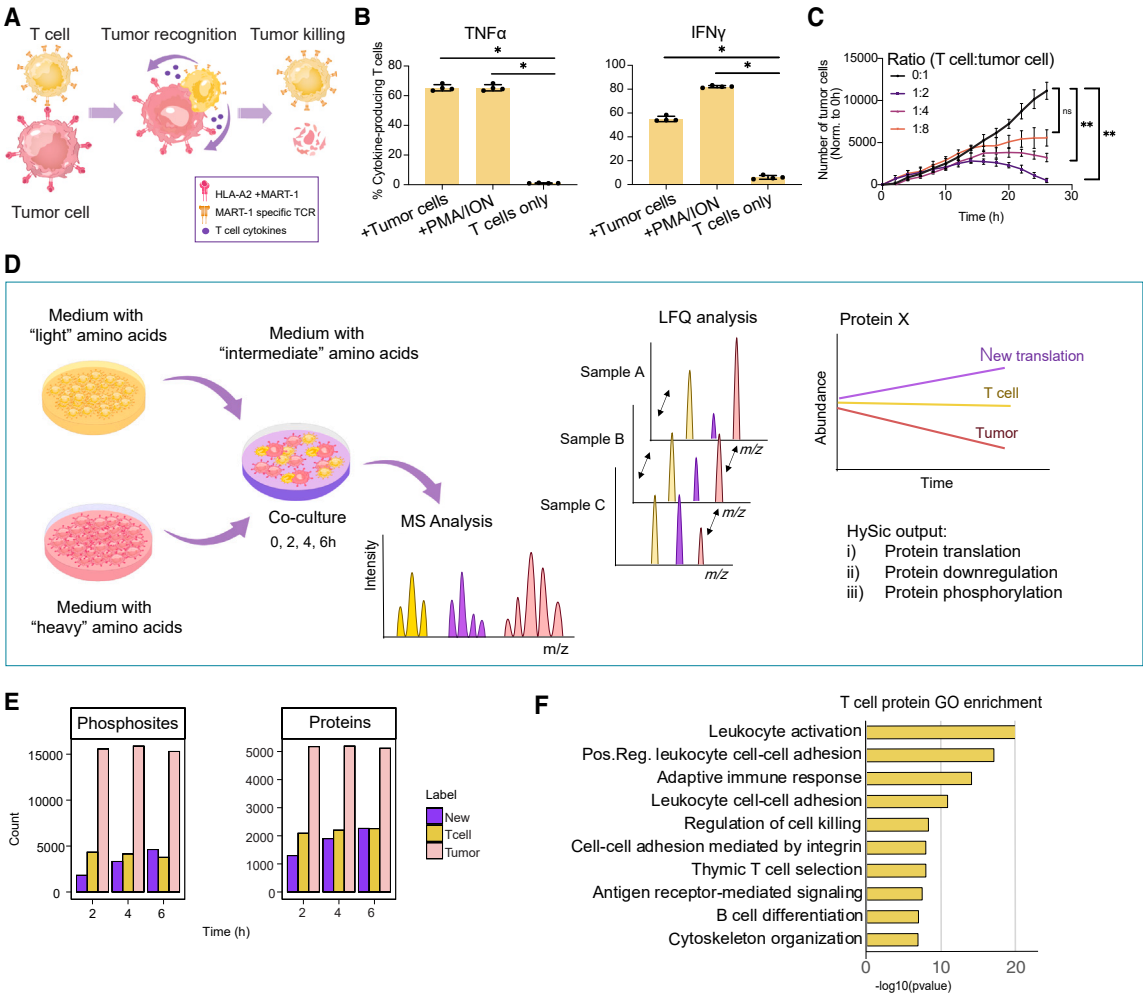

Figure 1. HySic: Hybrid quantification of SILAC-labeled interacting cells

(A) Schematic representation of T cell:tumor cell co-cultures. Tumor cells were transduced to express HLA-A2 and MART-1 antigen. T cells were isolated from peripheral blood mononuclear cells (PBMCs) from healthy donors and subsequently transduced with virus encoding a MART-1-specific TCR. Matched interactions lead to tumor cell recognition and killing by the T cells.

(B) T cell activation after 4.5 h co-culture as measured by TNF and IFNγ production by flow cytometry. Cells were co-cultured at 1:1 (T cell:tumor cell) ratio. As a positive control, T cells alone were cultured with PMA (50 μg/mL) and ionomycin (1 mg/mL). As a negative control, T cells were not stimulated. The y axis represents the percentage of cytokine-producing T cells. Each dot represents a technical replicate. Error bars represent SD. Mann-Whitney test was used for analysis.

(C) Cytotoxicity assay of tumor cells (EBC-1) and T cells co-cultured at different T cell ratios as indicated. Viability of tumor cells (expressing mPlum) was measured by Incucyte tumor cell count (red fluorescence counts) every 2 h. Data were normalized to 0 h. Error bars represent SD of 3 technical replicates. Statistical analysis was performed by Friedman test. $^{**}p < 0.01$, $^{****}p < 0.0001$.

(D) Schematic representation of HySic. T cells and tumor cells were labeled separately with "light" $^{0}K^{0}R$ or "heavy" $^{8}K^{10}R$ amino acids, respectively. Following complete label incorporation, the two cell types were co-cultured in medium with "intermediate" $^{4}K^{6}R$ amino acid isotopes. After 2, 4, and 6 h, cells were lysed and analyzed by MS. Samples were subsequently quantified by LFQ by comparing extracted ion chromatograms for each SILAC label independently. Protein information was annotated as T cells, tumor cells, or newly synthesized.

(E) Total count of quantified proteins and phosphosites by HySic with T cell, tumor cell, or newly synthesized label at the indicated time points.

(F) Top 10 enriched pathways of 242 proteins enriched in the T cell-labeled group. Proteins were selected for enrichment analysis if their expression in the T cell label at T0 was >2-fold higher than the tumor label across time points. Pathways are listed from smallest to largest p value. Enrichment of Gene Ontology (GO) biological processes was performed using Metascape.

bigger size (average 22.9 μm diameter compared to 6.9 μm of T cells). We also observed an increase in proteins and phosphoproteins in the newly synthesized channel over time, which was expected because of new protein translation. To confirm the specificity of our SILAC labels, we analyzed proteins that had higher abundance in the T cell-protein label and observed an enrichment in leukocyte activation, leukocyte cell-cell adhesion, and adaptive immune response, among other T cell-related pathways (Figure 1F). This result confirms that proteins detected in the T cell-protein label are of T cell origin, demonstrating the

specificity and efficiency of SILAC barcoding of the HySic differential labeling method. Enrichment analysis of tumor proteins showed no significant pathways, likely because the set of proteins is too generic.

HySic identifies interaction-induced newly synthesized proteins

We next used HySic to analyze the newly synthesized proteins, identified by the newly synthesized-protein label. To control for baseline translation, we compared the newly synthesized proteins in co-culture to individual incubation of tumor cells in newly synthesized-protein-label media for 4 h. We searched for proteins that were exclusively upregulated in the co-culture and extracted the newly synthesized proteins that were shared across cell lines for pathway enrichment analysis. Proteins were enriched in type II IFNγ and TNF signaling (Figures 2A and 2B), which is indicative of a TCR-antigen-MHC class I interaction triggering T cell secretion of IFNγ and TNF, causing subsequent tumor cell death.[19] These findings validate our ability to quantify expected biological responses using our HySic approach.

In co-cultures, the cell origin of newly synthesized proteins is unknown, as T cell- and tumor-cell-translated proteins share the newly synthesized-protein label. Therefore, the cell of origin of newly synthesized proteins needs to be validated with an independent technique. We selected IFNγ, CXCL10, ICAM1, and granzyme B (GZMB) and evaluated their protein expression in both cell types using flow cytometry (Figure 2C). After co-culturing, IFNγ and GZMB expression increased in T cells, whereas CXCL10 and ICAM1 expression increased in tumor cells (Figure 2D). However, GZMB protein expression was increased not only in T cells but also in tumor cells upon interaction with T cells, in agreement with a recent study.[20] These results were reproduced with an independent T cell donor in the four cell lines (Figure S2A). As a negative control, we evaluated proteins that did not show induced translation upon co-culture. We evaluated PD-L1, which was not increased upon T cell co-culture in three of the four tumor cell lines. We confirmed the absence of newly translated PD-L1 in those cell lines (Figure S2B). These findings were validated in an extended cell line panel including multiple cancer types (Figure S2C). Together, these data show that HySic in T cell:tumor cell co-cultures can be used to identify and quantify newly synthesized proteins upon cell:cell interactions.

T cell:tumor cell interactions promote turnover of CD8A and granulins

Another type of protein information obtained by HySic is protein downregulation. By labeling the proteins derived from either T cells or tumor cells, we can track their decrease during the co-culture in comparison to individual cell populations. We evaluated the T cell and tumor cell protein expression in co-culture over time. We normalized the data to cells cultured individually to correct for generic protein turnover. Then, the dataset was filtered for proteins, which were significantly downregulated (false discovery rate [FDR] < 0.15) relative to time point zero in at least one cell line and which showed downregulation across at least three out of four cell lines (Figures S3A and S3B). In this dataset, we observed cell-line-specific protein variation, which could be due to the different cancer subtypes used in this study (adenocarcinoma, squamous cell carcinoma, and large cell carcinoma). This was not unexpected in light of previous findings by us and others.[6,18,21] We performed pathway enrichment analysis to identify cellular processes affected by protein downregulation. Downregulated proteins in T cells were mainly enriched in immune system pathways, while in tumor cells they were enriched primarily in metabolic and RNA-processing pathways (Figure S3). We next filtered the data for proteins significantly decreasing and ranked by the average protein downregulation (Figures 3A and 3B). From the top 20 proteins with the largest average downregulation across all cell lines, we selected proteins for validation based on antibody availability: CD8 in T cells (top downregulated protein) and GRN in tumor cells (second-most downregulated protein). CD8 was previously shown to be downregulated upon TCR-antigen-MHC class I interaction.[22] To mimic the procedure of HySic, we pre-labeled CD8 with a flow cytometry antibody and co-incubated T cells and tumor cells for 6 h, after which the remaining labeled protein was measured. Indeed, CD8 protein levels were decreased after co-culture in four independent tumor cell lines (Figure 3C), validating the observations made and illustrating the quantitative power of HySic. These results were reproduced with an independent T cell donor (Figure S3D) and validated in a larger cell line panel (Figure S3E). Using an alternative approach, we evaluated GRN protein expression in tumor cells by western blotting before and after co-culture with T cells. We observed a decrease in GRN expression in the cell line panel co-cultured with T cells from three donors (Figures 3D, and S3F), which validates the HySic findings. These results were reproduced in a larger tumor cell line panel comprising different cancer types (Figure S3F and S3G).

HySic identifies induced RHO/RAC/PAK1 signaling upon T cell:tumor cell interactions

In addition to protein translation and degradation, HySic allows for the measurement of phosphorylation dynamics between and within interacting cells. Protein phosphorylation is the most common PTM, and it heavily influences the function of proteins and protein networks.[11,23] Therefore, we set out to establish which cellular processes are changed upon cell:cell interactions at the phosphorylation level within T cells, tumor cells, and in newly translated proteins. We first examined the newly synthesized phosphoproteins and found 70 phosphosites upregulated >2-fold above background translation at later time points (4 and 6 h) in at least three of four co-cultured cell lines (Figure S4A). These phosphorylated proteins showed high enrichment for factors associated with TNF signaling (Figure S4B), which can be explained by the important role of TNF in mediating immune cell cytotoxicity. This finding contrasts with the IFNG pathway that was mainly enriched at the level of protein translation (Figure 2B). Taken together, these data demonstrate the unique layers of information that can be revealed by the combination of proteome and phosphoproteome data.

We next performed a hierarchical clustering of the significantly regulated phosphorylation sites for T cells and tumor cells that were shared across at least three out of four cell lines for tumor proteins, or shared across both T cell donors for T cell proteins (Figure 4A). The clusters containing increased phosphorylation

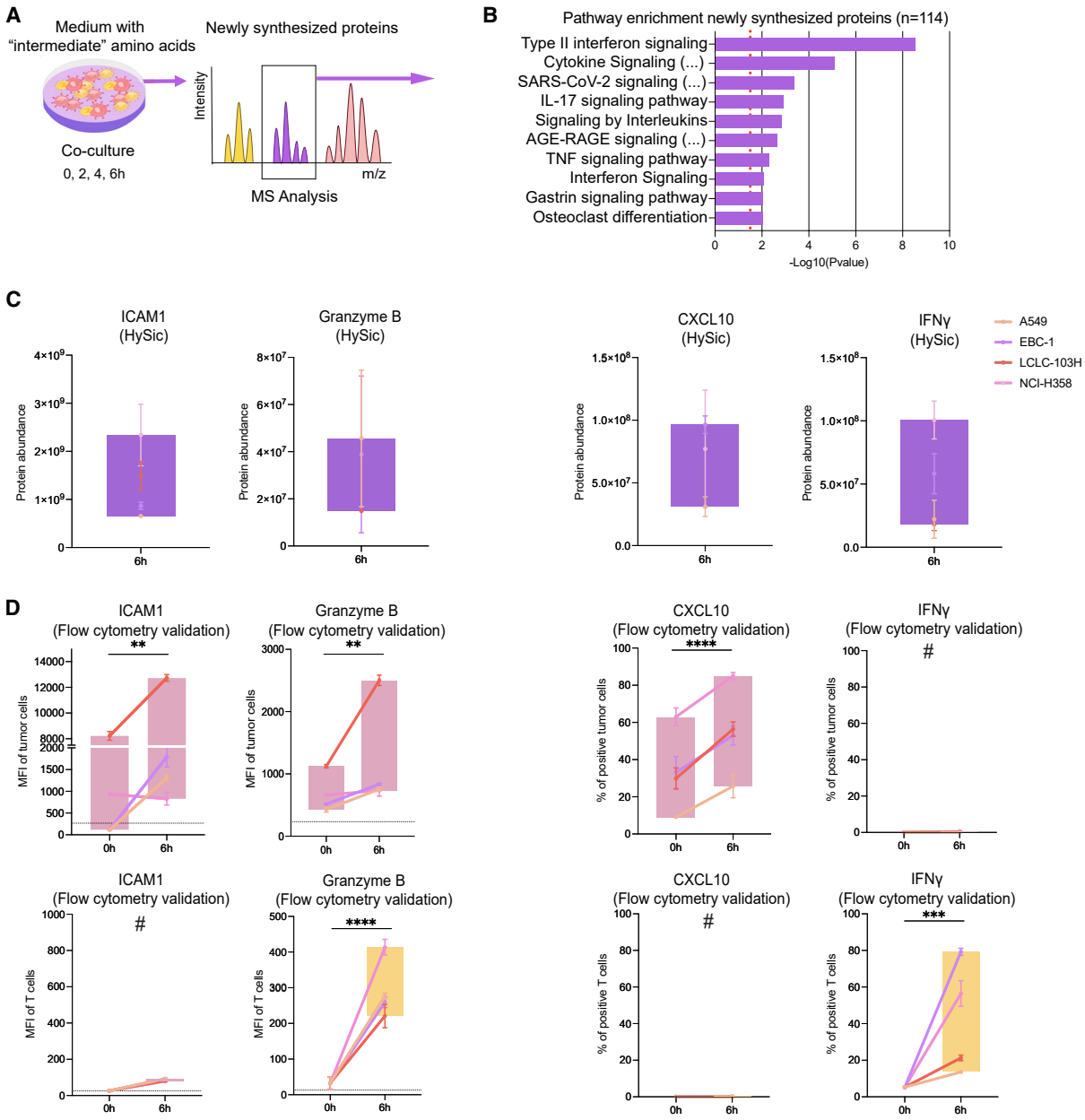

Figure 2. HySic identifies interaction-induced newly synthesized proteins

(A) Schematic representation of newly synthesized protein measurements by HySic.

(B) HySic top 10 enriched pathways in proteins detected in the channel for newly synthesized proteins. Enrichment was performed using *Gprofiler* with Reactome and WikiPathways databases. Pathways are listed from smallest to largest p value.

(C) Protein abundance detected by HySic of the indicated proteins. Each cell line is represented by a colored dot with SD bars. Boxplots indicate deviation of four cell lines combined.

(D) Median fluorescence intensity (MFI) or percentage of positive cells measured by flow cytometry of the indicated proteins in either tumor cells (pink boxplots) or T cells (yellow boxplots). Each cell line is represented by a colored dot with SD bars. Boxplots indicate deviation of four cell lines combined. $^{**}p < 0.01$, $^{***}p < 0.001$, $^{****}p < 0.0001$. Two-way ANOVA test used for statistical analysis. A hash symbol (#) indicates below detection levels determined by the unstained sample.

were analyzed for pathway enrichment. The T cells and tumor cells revealed a shared pathway enriched for RHO/RAC signaling (Figure 4B). The cluster containing decreased phosphorylation showed similar pathways enriched (Figure S4C). RHO/RAC signaling includes multiple downstream cellular processes, many of which are linked to both cancer progression[24,25] and T cell migration and activation.[26] There are five major downstream RHO/RAC effector proteins: ROCK (1–2), PAK (1–6), mDia, WASP,

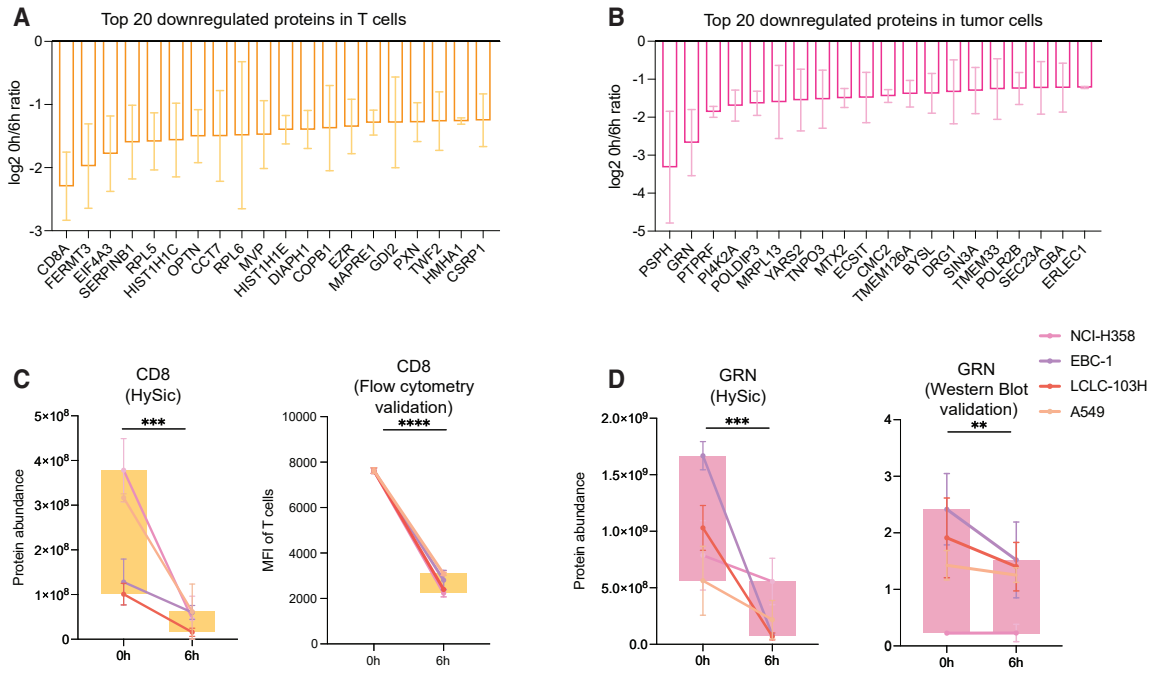

Figure 3. T cell:tumor cell interactions promote turnover of CD8A and granulins

(A) Rank of top 20 downregulated proteins selected in T cells shown on the x axis. Proteins were filtered for FDR <0.15 in at least one out of four cell lines. FDR significance was determined by Benjamini-Hochberg correction of unpaired t test p values. Then, proteins were ranked based on average effect size across all cell lines. Each dot represents a cell line, and errors bars represent SEM. The y axis represent log2 0/6 h protein expression ratio.

(B) Rank of top 20 downregulated proteins selected in tumor cells shown on the x axis. Proteins were filtered for FDR <0.15 in at least one out of four cell lines. FDR significance was determined by Benjamini-Hochberg correction of unpaired t test p values. Then, proteins were ranked based on average effect size across all cell lines. Each dot represents a cell line, and errors bars represent SEM. The y axis represents log2 0/6 h protein expression ratio.

(C) Abundance of CD8 protein detected by HySic (left) or flow cytometry validation (right). MFI measured by flow cytometry. Each cell line is represented by a colored dot with SD bars. Boxplot indicates deviation of four cell lines combined. ***p < 0.001, ****p < 0.0001. Two-way ANOVA test used for statistical analysis.

(D) Abundance of GRN protein detected by HySic (left) or western blot validation (right). Protein expression normalized to vinculin is quantified. Each cell line is represented by a colored dot with SD bars. Boxplot indicates deviation of four cell lines combined tested with three T cell donors. **p < 0.01, ***p < 0.001. Two-way ANOVA test used for statistical analysis.

and WAVE.[27] To understand which of these may account for the downstream signaling in our model, we analyzed the phosphorylation status of the five candidates upon T cell:tumor cell co-culture in four tumor cell lines (from which phosphosites were detected in MS). The phosphorylation coverage of several candidate effector proteins was sparse and showed varied patterns of regulation. However, among all tested proteins, PAK1-activating sites (pS144, pS174, pT212, pS223) were consistently more phosphorylated upon T cell:tumor cell interactions (Figure 4C). WAVE also showed activating phosphosites upregulated across different cell lines. Conversely, ROCK1 showed decreased phosphorylation of the activating site pS1341.

To explore whether the phosphorylation of activating sites in PAK1 and the other effector proteins could have clinical relevance, we analyzed the same phosphosites in a lung cancer clinical study, which includes phosphoproteomics of tumor and healthy normal tissue.[28] PAK1-activating phosphosites were more abundant in tumor compared to healthy tissue (Figures 4D and S4D). This was reproduced in an independent lung cancer cohort[29] (Figure S4E). ROCK1-activating phosphorylation was, by contrast, lower in tumor vs. healthy tissue, following the trend observed in T cell:tumor cell co-cultures. The remaining effector proteins with available data were also evaluated, but no consistent trends were observed (Figures S4D and S4E). The increase in activating phosphorylation in PAK1 upon T cell:tumor cell engagement led us to investigate PAK1 as a possible target in tumor immunotherapy.

PAK1 inhibition enhances tumor cell sensitivity to T cells

PAK1 has been previously studied in cancer,[30–34] but its role in the context of cytotoxic T cell killing is less studied. Therefore, we first wished to increase our understanding of the role of PAK1 in T cells and, second, evaluate its action in T cell:tumor co-cultures. To inhibit PAK1 activity, we treated T cells with a selective inhibitor (NVS-PAK1) (Figure S5A). We first evaluated the on-target effect of the inhibitor by phosphoproteomic analysis of T cells treated for 1 or 5 days with NVS-PAK1. We observed a decrease in the PAK1 autophosphorylation site pS144 (Figure S5B). This phosphosite serves as a positive control for PAK1 inhibition, as PAK1 must be functional to perform S144 autophosphorylation.[35] We next analyzed protein expression changes in T cells upon a 5-day NVS-PAK1 treatment. At the proteomic level, we observed an increase in the T cell-derived cytotoxic protein GZMB

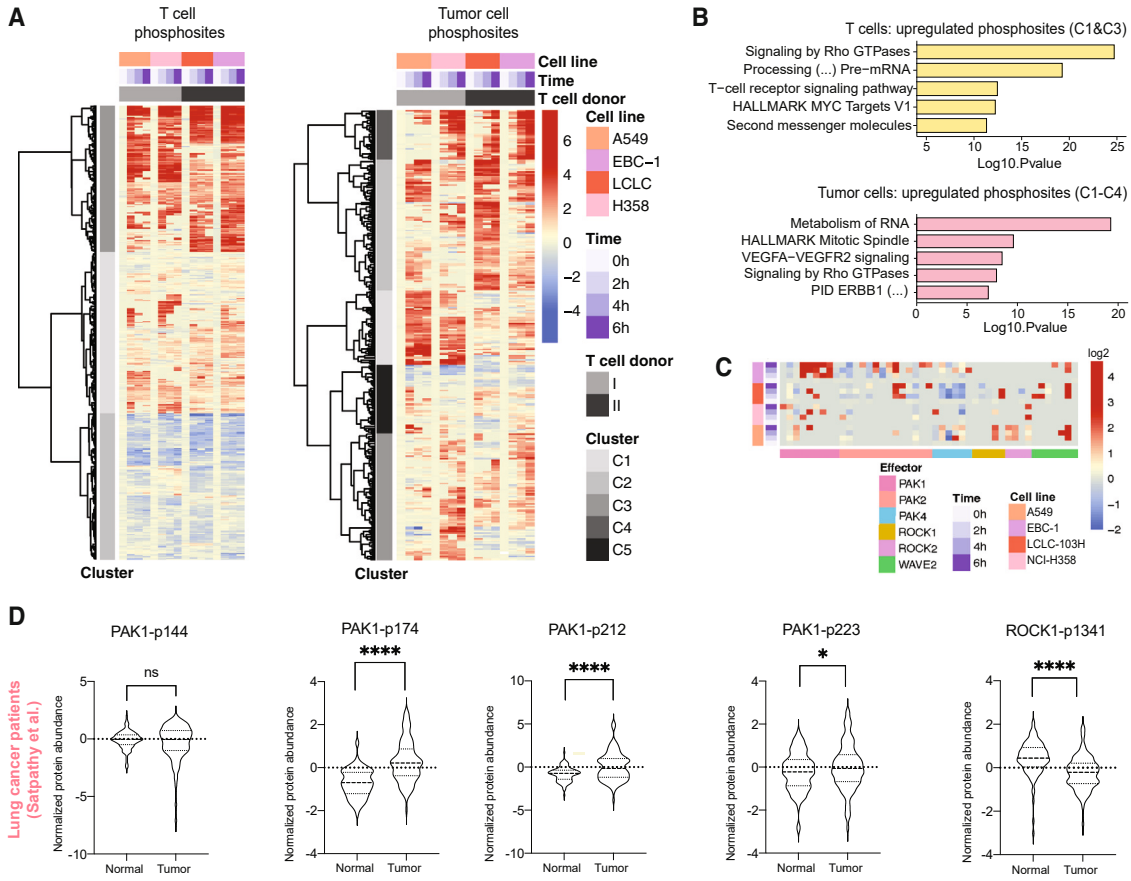

Figure 4. T cell:tumor cell interaction upregulates RHO/RAC signaling and PAK1 activation phosphosites, which are increased in tumor vs. healthy tissue

(A) Significantly regulated phosphosites (FDR < 0.15) shared across both T cell donors for T cells (left, 439 phosphosites) and at least in 3/4 cell lines for tumor cells (right, 310 phosphosites). FDR significance was determined by Benjamini-Hochberg correction of one-way ANOVA p values. Phosphosite expression values represent log2 T0-normalized data. Missing values are replaced with zero for heatmap clustering.

(B) Pathway enrichment (by Metascape) for upregulated phosphorylated proteins from phosphosite heatmap clusters in T cells (C1 and C3, 241 unique phosphorylated proteins) and tumor cells (C1–C4, 223 unique phosphorylated proteins). The top five enrichment terms are displayed.

(C) Heatmap clustering of log2 T0-normalized RHO/RAC effector protein phosphorylation sites. Missing values are replaced with zero for heatmap visualization.

(D) Normalized phosphosite abundance from Satpathy et al.[28] of the indicated protein sites in healthy (normal) vs. tumor tissue. Violin plots represent average of individual patient expressions. Wilconxon paired test was used for statistical analysis.

(Figure 5A). We validated the increase in GZMB protein expression by flow cytometry upon treatment with NVS-PAK1, as well with a second PAK1 inhibitor, FRAX-597 (Figures 5B and S5C). In addition, we evaluated the effect of PAK1 inhibition on T cells by analyzing T cell activation markers by flow cytometry. Activation markers CD69 and CD137 were increased upon NVS-PAK1 treatment in T cells (Figure S5D). Thus, PAK1 inhibition on T cells increases the production of the cytotoxic molecule GZMB and increases the expression of cell surface activation markers.

Lastly, we set out to determine whether PAK1 inhibition would have a beneficial effect on T cell-mediated tumor killing. T cells and tumor were co-cultured and treated with NVS-PAK1 at various T cell:tumor ratios in a time course analysis in four independent cell lines. NVS-PAK1 treatment significantly increased tumor sensitivity to T cell killing in three out of the four NSCLC cell lines tested (Figure 5C). The effect of this drug was additive to T cell killing in two NSCLC cell lines (score <10 in EBC-1 and NCI-H358) and synergistic in the third cell line (score >10 in LCLC-103H) as evaluated by Synergyfinder.[36] In the fourth cell line, there was no additive nor synergistic effect observed (Figures 5D and S5E). To extend these findings to other cancer types, we repeated the experiment in breast, colon, and prostate cancer cell lines. NVS-PAK1 again significantly increased T cell killing sensitivity in colon and prostate cancer cell lines but not in the breast cancer cell line (Figures 5E and S5F). Together, these data indicate that PAK1 inhibition can enhance the sensitivity of tumor cells to T cell killing in multiple cancer types, including NSCLC and colon and prostate cancers.

DISCUSSION

Deciphering the complex signaling networks that mediate the defense of tumor cells against T cell attack requires comprehensive

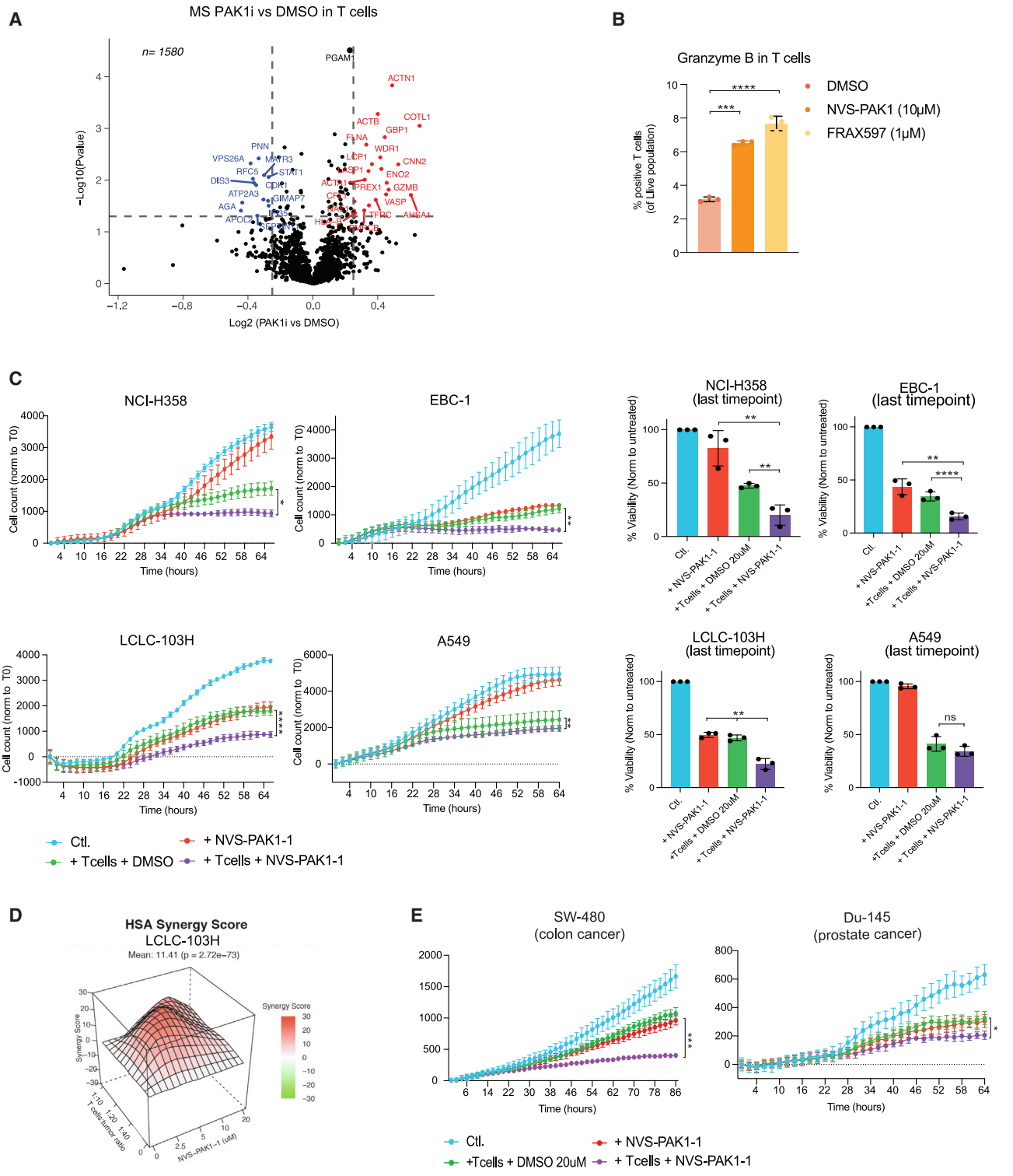

Figure 5. Inhibition of PAK1 increases T cell sensitivity

(A) Proteome profiling of NVS-PAK1-treated (10 μM, 5 days) vs. DMSO-treated T cells for 5 days. Colored dots are significantly increased (red) or decreased (blue) by NVS-PAK1 treatment ($p < 0.05$; unpaired t test) with a log2 fold change > 0.25.

(B) Percentage of granzyme-B-positive T cells (of live population) upon treatment with NVS-PAK1 (10 μM), FRAX587 (1 μM), or DMSO for 5 days. ***$p < 0.001$, ****$p < 0.0001$. Two-way ANOVA test used for statistical analysis.

(legend continued on next page)

analyses, particularly at the protein level. However, such (phospho)proteomic studies have been limited owing to the technical challenge of preserving cell-type-specific information in a mixed-cell system. Here, we have developed a method to determine rapid protein translation and phosphorylation dynamics in interacting T cells and tumor cells: HySic. Although previous studies performed proteomics of interacting cells, mainly by the use of SILAC,[16,17,37] they either made use of physical cell:cell separations or did not study the individual cell types involved in the interaction. Therefore, we developed a workflow allowing for SILAC-labeled cells to interact without the need of a physical separation step, leaving the (phospho)proteome landscape unaltered. We simultaneously analyzed proteins and phosphosites derived from both T cells and tumor cells, as well as the proteins that were newly translated at the time of their interactions. SILAC was used to identify the origin of a given protein/phosphosite, followed by label-free quantification of the individual SILAC-labeled peptides. This combined data analysis allowed us to track protein and phosphosite dynamics over different cell types, amounts of time, and treatment conditions. We validated data for protein translation and degradation obtained by HySic, while our integrative phosphoproteomics analysis identified PAK1 as a potential target for tumor sensitization to T cell killing.

As one aspect of our method, we studied protein degradation upon T cell:tumor interaction. We identified proteins that were downregulated upon cell interaction, and several were selected for validation. As an expected event, we observed the turnover of CD8 in T cells upon T cell:tumor cell interaction.[22] On the tumor cell side, we observed the downregulation of GRN. Recently, it has been shown that the granulin precursor (Pro-granulin) can induce PD-L1 and that blocking Pro-granulins can sensitize tumors to T cell killing in an immunocompetent mouse model.[38,39] The mechanisms behind the downregulation of these and other proteins in interacting T cells and tumor cells remain to be studied in more detail. Furthermore, in this study, we did not investigate how the effect size of downregulated or inhibited proteins translates into different cell biology. These are protein-specific features; for example, to achieve clinically meaningful inhibition of BRAF kinase, deep target blockade is required,[40] whereas partial loss of p53 can already have profound effects, allowing for tumorigenic events.[41]

In addition to protein translation and turnover, HySic enables the quantification of cell-specific phosphoproteomics data. Following co-culture, T cells and tumor cells are snap frozen together without additional perturbation caused by cell-separation methods, which can profoundly influence phosphorylation dynamics. This allows capturing more transient phosphosites that could change within seconds otherwise.[42] By analyzing the most abundant changes in the phosphoproteome of both T cells and tumor cells, we found a shared pathway being altered during cell-cell engagement: RHO/RAC signaling. This pathway is broadly involved in cell-cell communication via modulation of the cell cytoskeleton, among other functions[43] One of its effector proteins, PAK1, has been thoroughly studied in tumor cells. We observed that activating phosphosites of PAK1 were increased in tumor vs. adjacent healthy tissue in patients with cancer. However, considerably less is known about the role of PAK1 in T cells or in the context of T cell:tumor interactions. By pharmacologically inhibiting PAK1, we uncovered new properties associated with this effector protein in T cells: induction of GZMB and increased expression of activation proteins. Furthermore, we show that PAK1 inhibition increases tumor sensitivity to T cell killing. This sensitization effect is additive to that of T cells in two cell lines (EBC-1 and NCI-H358), synergistic in one cell line (LCLC-103H), and non-significant in the fourth (A549). The mechanism behind PAK1 inhibition on both T cells and tumor cells merits further study.

PAK1 is already being considered as an attractive oncological target due to its contribution to several oncogenic signaling pathways in cancer cells.[33] Most described PAK1 inhibitors target also other PAK family members, which can lead to toxicity. Recently, a more selective inhibitor (NVS-PAK1, used in this study) was developed, but its efficacy in an *in vivo* Schwannoma mouse model was limited.[44] Future development of an efficient and selective PAK1 inhibitor could help to translate our findings in pre-clinical models. In addition, 3/4 PAK1-activating sites have a higher phosphorylation degree in tumor tissue compared to healthy tissue in two cohorts. However, these data show high variation and lack functional insights. Therefore, the data presented here suggest that PAK1 may be a valuable target, but further pre-clinical testing will be required. Following the functional validation of PAK1, other phosphoprotein pathways described may also be explored to boost mechanisms of tumor sensitivity to T cells.

An important consideration for our method is that co-culture incubation times using the HySic approach must be kept short (<8 h) to avoid extensive proteome mixing due to protein turnover. To avoid proteome mixing in SILAC co-cultures, cell lines can be genetically engineered to uniquely metabolize and incorporate amino acid precursors.[45] This approach has been successful for delineating translation in mixed cell cultures. However, it requires an extensive experimental setup involving exogenous expression of metabolic enzymes, which can be difficult to implement, especially in primary cells like T cells.

(C) (Left) Cytotoxic assay of tumor and T cells co-cultured with or without NVS-PAK1 in Incucyte. Inhibitor concentration and T cell:tumor ratio were optimized for each cell line: NCI-H358 (2.5 μM and 1:20), EBC-1 (10μM and 1:10), LCLC-103H (5 μM and 1:10), and A549 (2.5 μM and 1:10). Viability of tumor cells (expressing mPlum) was measured by red fluorescence counts every 2 h. Data were normalized to 0 h. Error bars represent SD of 3 technical replicates. Statistical analysis was performed by Friedman test. *$p < 0.05$, **$p < 0.01$, ****$p < 0.0001$. (Right) Endpoints of experiments shown on the left, normalized to untreated control. Each dot represents a technical replicate, and error bars represent SD. Nested T test was used for statistical analysis. **$p < 0.01$, ****$p < 0.0001$.

(D) Synergy score (HSA) calculated with *Synergyfinder* on the indicated T cell:tumor cell ratios and drug concentrations for LCLC-103H cells. Score indicates the percentage of additive effect of using a combination of two treatments compared to the single agents.

(E) Cytotoxic assay of T cells and tumor cells co-cultured with or without NVS-PAK1 in an Incucyte. Inhibitor concentration and T cell:tumor ratio were optimized per cell line: SW-480 (20 μM, 1:10) and DU-145 (10 μM, 1:10). Data were normalized to 0 h. Error bars represent SD of 3 technical replicates. Statistical analysis was performed by Friedman test. *$p < 0.05$, ***$p < 0.001$.

Therefore, we view HySic as a simple and easy alternative for studies prioritizing rapid signaling dynamics between interacting cells.

In conclusion, we have established HySic as an MS method to identify protein and phosphoprotein changes in SILAC-labeled interacting cells. After validation of the technique, we have explored its possibilities: HySic allowed identifying newly translated and downregulated proteins, as well as mapping phosphoprotein dynamics. The latter option enabled us to identify and explore PAK1 as a target whose inhibition increases tumor cell sensitivity to T cells. Beyond PAK1, other pathways and actionable targets also emerged from our dataset, meriting further investigation. Thus, HySic is a relatively easy method that can retrieve extensive functional protein data in different types of cell co-cultures.

Limitations of the study

This study has some limitations that should be considered. Although HySic allows for identifying proteins that are synthesized during heterotypic cell:cell interactions, they are labeled with the same isotopes. Therefore, additional analyses will be required to annotate such proteins to the cell type of origin. Of note, this is not a problem for protein phosphorylation and downregulation of existing T cell and tumor proteins. Furthermore, HySic does not allow for quantifying the turnover rate of newly translated proteins, as the measurements reflect steady-state abundances. This consideration may be important for proteins with rapid turnover rates. Lastly, our identification of PAK1 as a possible target to sensitize tumor cells to T cell killing needs further mechanistic insight and improved inhibitors for pre-clinical exploration.

STAR★METHODS

Detailed methods are provided in the online version of this paper and include the following:

SUPPLEMENTAL INFORMATION

Supplemental information can be found online at https://doi.org/10.1016/j.celrep.2023.113598.

ACKNOWLEDGMENTS

We would like to thank the Schumacher lab for sharing the MART-1 TCR system. We thank our colleagues in the lab and division for valuable input and discussion and Nils Visser for technical support. We would also like to thank the flow cytometry facility in NKI-AVL for contributing to this work. This work received support from the Horizon 2020 program INFRAIA project Epic-XS (Project 823839) and the NWO-funded Netherlands Proteomics Center through the National Road Map for Large-scale Infrastructures program X-Omics (Project 184.034.019). F.W. is partially funded by the China Scholarship Council no. 202009370061. D.S.P. is funded by, and is a member of, the Oncode Institute, which is partly financed by the Dutch Cancer Society.

AUTHOR CONTRIBUTIONS

S.I.-M., M.A., D.S.P., and K.E.S. conceived the study and designed the experiments. S.I.-M., J.T.M.P., A.A., and A.M.T. performed cell culture experiments. F.W. and K.E.S. performed MS analysis. S.I.-M. and K.E.S. performed bioinformatic analysis. S.I.-M., D.S.P., and K.E.S. wrote the manuscript. All authors read and approved the manuscript. The project was supervised by M.A. and D.S.P.

DECLARATION OF INTERESTS

S.I.-M. and D.S.P. are named inventors on patent P097110NL, which is unrelated to this work. D.S.P. is co-founder, shareholder, and advisor of Immagene, which is unrelated to this work. M.A. is currently lead scientific officer for Amigon, which has no relation to this work.

Received: May 30, 2023
Revised: September 16, 2023
Accepted: December 4, 2023
Published: December 26, 2023

REFERENCES

1. Hellmann, M.D., Paz-Ares, L., Bernabe Caro, R., Zurawski, B., Kim, S.W., Carcereny Costa, E., Park, K., Alexandru, A., Lupinacci, L., de la Mora Jimenez, E., et al. (2019). Nivolumab plus Ipilimumab in Advanced Non–Small-Cell Lung Cancer. N. Engl. J. Med. *381*, 2020–2031.
2. Sharma, P., Hu-Lieskovan, S., Wargo, J.A., and Ribas, A. (2017). Primary, Adaptive, and Acquired Resistance to Cancer Immunotherapy. Cell *168*, 707–723.
3. Kalbasi, A., and Ribas, A. (2020). Tumour-intrinsic resistance to immune checkpoint blockade. Preprint at Nature Reviews Immunology *20*, 25–39.
4. Vredevoogd, D.W., Apriamashvili, G., and Peeper, D.S. (2021). The (re)discovery of tumor-intrinsic determinants of immune sensitivity by functional genetic screens. Preprint at Immuno-Oncology and Technology *11*.
5. Kearney, C.J., Vervoort, S.J., Hogg, S.J., Ramsbottom, K.M., Freeman, A.J., Lalaoui, N., Pijpers, L., Michie, J., Brown, K.K., Knight, D.A., et al. (2018). Tumor immune evasion arises through loss of TNF sensitivity. Sci. Immunol. *3*, eaar3451.
6. Vredevoogd, D.W., Kuilman, T., Ligtenberg, M.A., Boshuizen, J., Stecker, K.E., de Bruijn, B., Krijgsman, O., Huang, X., Kenski, J.C.N., Lacroix, R., et al. (2019). Augmenting Immunotherapy Impact by Lowering Tumor TNF Cytotoxicity Threshold. Cell *178*, 585–599.e15.

7. Zhang, Z., Kong, X., Ligtenberg, M.A., van Hal-van Veen, S.E., Visser, N.L., de Bruijn, B., Stecker, K., van der Helm, P.W., Kuilman, T., Hoefsmit, E.P., et al. (2022). RNF31 inhibition sensitizes tumors to bystander killing by innate and adaptive immune cells. Cell Rep. Med. *3*, 100655.
8. Boulos, J.C., Yousof Idres, M.R., and Efferth, T. (2020). Investigation of cancer drug resistance mechanisms by phosphoproteomics. Pharmacol. Res. *160*, 105091.
9. Tocheva, A.S., Peled, M., Strazza, M., Adam, K.R., Lerrer, S., Nayak, S., Azoulay-Alfaguter, I., Foster, C.J.R., Philips, E.A., Neel, B.G., et al. (2020). Quantitative phosphoproteomic analysis reveals involvement of PD-1 in multiple T cell functions. J. Biol. Chem. *295*, 18036–18050.
10. Ruperez, P., Gago-Martinez, A., Burlingame, A.L., and Oses-Prieto, J.A. (2012). Quantitative phosphoproteomic analysis reveals a role for serine and threonine kinases in the cytoskeletal reorganization in early T cell receptor activation in human primary T cells. In Molecular and Cellular Proteomics.
11. Ardito, F., Giuliani, M., Perrone, D., Troiano, G., and Lo Muzio, L. (2017). The crucial role of protein phosphorylation in cell signalingand its use as targeted therapy (Review). Int. J. Mol. Med. *40*, 271–280.
12. Riley, N.M., and Coon, J.J. (2016). Phosphoproteomics in the Age of Rapid and Deep Proteome Profiling. Anal. Chem. *88*, 74–94.
13. Urban, J. (2022). A review on recent trends in the phosphoproteomics workflow. From sample preparation to data analysis. Anal. Chim. Acta *1199*, 338857.
14. Ong, S.E., Blagoev, B., Kratchmarova, I., Kristensen, D.B., Steen, H., Pandey, A., and Mann, M. (2002). Stable isotope labeling by amino acids in cell culture, SILAC, as a simple and accurate approach to expression proteomics. Mol. Cell. Proteomics *1*, 376–386.
15. Ibarrola, N., Kalume, D.E., Gronborg, M., Iwahori, A., and Pandey, A. (2003). A Proteomic Approach for Quantitation of Phosphorylation Using Stable Isotope Labeling in Cell Culture. Anal. Chem. *75*, 6043–6049.
16. Griffith, A.A., Callahan, K.P., King, N.G., Xiao, Q., Su, X., and Salomon, A.R. (2022). SILAC Phosphoproteomics Reveals Unique Signaling Circuits in CAR-T Cells and the Inhibition of B Cell-Activating Phosphorylation in Target Cells. J. Proteome Res. *21*, 395–409.
17. Liu, R., Wang, Y., Li, B., Wang, H., Guan, F., Tan, Z., and Li, X. (2019). Screening differentially expressed proteins from co-cultured hematopoietic cells and bone marrow-derived stromal cells by quantitative proteomics (Silac) method. Clin. Proteonomics *16*, 32.
18. Ibáñez-Molero, S., van Vliet, A., Pozniak, J., Hummelink, K., Terry, A.M., Monkhorst, K., Sanders, J., Hofland, I., Landeloos, E., Van Herck, Y., et al. (2022). SERPINB9 is commonly amplified and high expression in cancer cells correlates with poor immune checkpoint blockade response. OncoImmunology *11*, 2139074.
19. Jorgovanovic, D., Song, M., Wang, L., and Zhang, Y. (2020). Roles of IFN-γin tumor progression and regression: A review. Preprint at Biomarker Research *8*, 1–16.
20. Jiang, L., Wang, Y.J., Zhao, J., Uehara, M., Hou, Q., Kasinath, V., Ichimura, T., Banouni, N., Dai, L., Li, X., et al. (2020). Direct Tumor Killing and Immunotherapy through Anti-SerpinB9 Therapy. Cell *183*, 1219–1233.e18.
21. Gonçalves, E., Poulos, R.C., Cai, Z., Barthorpe, S., Manda, S.S., Lucas, N., Beck, A., Bucio-Noble, D., Dausmann, M., Hall, C., et al. (2022). Pan-cancer proteomic map of 949 human cell lines. Cancer Cell *40*, 835–849.
22. Xiao, Z., Mescher, M.F., and Jameson, S.C. (2007). Detuning CD8 T cells: Down-regulation of CD8 expression, tetramer binding, and response during CTL activation. J. Exp. Med. *204*, 2667–2677.
23. Pawson, T., and Scott, J.D. (2005). Protein phosphorylation in signaling - 50 Years and counting. In Trends in Biochemical Sciences.
24. Lin, Y., and Zheng, Y. (2015). Approaches of targeting Rho GTPases in cancer drug discovery. Preprint at Expet Opin. Drug Discov. *10*, 991–1010.
25. Clayton, N.S., and Ridley, A.J. (2020). Targeting Rho GTPase Signaling Networks in Cancer. Preprint at Frontiers in Cell and Developmental Biology *8*.
26. Saoudi, A., Kassem, S., Dejean, A., and Gaud, G. (2014). Rho-GTPases as key regulators of T lymphocyte biology. Small GTPases *5*, e28208.
27. Møller, L.L.V., Klip, A., and Sylow, L. (2019). Rho GTPases—Emerging Regulators of Glucose Homeostasis and Metabolic Health. Cells *8*, 434.
28. Satpathy, S., Krug, K., Jean Beltran, P.M., Savage, S.R., Petralia, F., Kumar-Sinha, C., Dou, Y., Reva, B., Kane, M.H., Avanessian, S.C., et al. (2021). A proteogenomic portrait of lung squamous cell carcinoma. Cell *184*, 4348–4371.e40.
29. Gillette, M.A., Satpathy, S., Cao, S., Dhanasekaran, S.M., Vasaikar, S.V., Krug, K., Petralia, F., Li, Y., Liang, W.W., Reva, B., et al. (2020). Proteogenomic Characterization Reveals Therapeutic Vulnerabilities in Lung Adenocarcinoma. Cell *182*, 200–225.e35.
30. Chung, J.H., Kim, T., Kang, Y.J., Yoon, S.H., Kim, Y.S., Lee, S.K., Son, J.H., Son, B., and Kim, D.H. (2020). Pak1 as a potential therapeutic target in male smokers with egfr-mutant non-small cell lung cancer. Molecules *25*, 5588.
31. Liu, H., Liu, K., and Dong, Z. (2021). The Role of p21-Activated Kinases in Cancer and Beyond: Where Are We Heading?. Preprint at Frontiers in Cell and Developmental Biology *9*.
32. Wang, K., Zhan, Y., Huynh, N., Dumesny, C., Wang, X., Asadi, K., Herrmann, D., Timpson, P., Yang, Y., Walsh, K., et al. (2020). Inhibition of PAK1 suppresses pancreatic cancer by stimulation of anti-tumour immunity through down-regulation of PD-L1. Cancer Lett. *472*, 8–18.
33. Semenova, G., and Chernoff, J. (2017). Targeting PAK1. Preprint at Biochemical Society Transactions *45*, 79–88.
34. Chow, H.-Y., Karchugina, S., Groendyke, B.J., Toenjes, S., Hatcher, J., Donovan, K.A., Fischer, E.S., Abalakov, G., Faezov, B., Dunbrack, R., et al. (2022). Development and utility of a PAK1-selective degrader. Preprint at bioRxiv.
35. Chong, C., Tan, L., Lim, L., and Manser, E. (2001). The mechanism of PAK activation. Autophosphorylation events in both regulatory and kinase domains control activity. J. Biol. Chem. *276*, 17347–17353.
36. Ianevski, A., Giri, K.A., and Aittokallio, T. (2022). SynergyFinder 3.0: an interactive analysis and consensus interpretation of multi-drug synergies across multiple samples. Nucleic Acids Research, gkac382.
37. Ramello, M.C., Benzaïd, I., Kuenzi, B.M., Lienlaf-Moreno, M., Kandell, W.M., Santiago, D.N., Pabón-Saldaña, M., Darville, L., Fang, B., Rix, U., et al. (2019). An immunoproteomic approach to characterize the CAR interactome and signalosome. Sci. Signal. *12*, eaap9777.
38. Fang, W., Zhou, T., Shi, H., Yao, M., Zhang, D., Qian, H., Zeng, Q., Wang, Y., Jin, F., Chai, C., and Chen, T. (2021). Progranulin induces immune escape in breast cancer via up-regulating PD-L1 expression on tumor-associated macrophages (TAMs) and promoting CD8+ T cell exclusion. J. Exp. Clin. Cancer Res. *40*, 4.
39. Cheung, P.F., Yang, J., Fang, R., Borgers, A., Krengel, K., Stoffel, A., Althoff, K., Yip, C.W., Siu, E.H.L., Ng, L.W.C., et al. (2022). Progranulin mediates immune evasion of pancreatic ductal adenocarcinoma through regulation of MHCI expression. Nat. Commun. *13*, 156.
40. Bollag, G., Hirth, P., Tsai, J., Zhang, J., Ibrahim, P.N., Cho, H., Spevak, W., Zhang, C., Zhang, Y., Habets, G., et al. (2010). Clinical efficacy of a RAF inhibitor needs broad target blockade in BRAF-mutant melanoma. Nature *467*, 596–599.
41. Kemp, C.J., Donehower, L.A., Bradley, A., and Balmain, A. (1993). Reduction of p53 gene dosage does not increase initiation or promotion but enhances malignant progression of chemically induced skin tumors. Cell *74*, 813–822.
42. Blazek, M., Santisteban, T.S., Zengerle, R., and Meier, M. (2015). Analysis of fast protein phosphorylation kinetics in single cells on a microfluidic chip. Lab Chip *15*, 726–734.
43. Burridge, K., and Wennerberg, K. (2004). Rho and Rac Take Center Stage. Preprint at Cell *116*, 167–179.
44. Hawley, E., Gehlhausen, J., Karchugina, S., Chow, H.Y., Araiza-Olivera, D., Radu, M., Smith, A., Burks, C., Jiang, L., Li, X., et al. (2021). PAK1 inhibition reduces tumor size and extends the lifespan of mice in a genetically engineered mouse model of Neurofibromatosis Type 2 (NF2). Hum. Mol. Genet. *30*, 1607–1617.

45. Gauthier, N.P., Soufi, B., Walkowicz, W.E., Pedicord, V.A., Mavrakis, K.J., Macek, B., Gin, D.Y., Sander, C., and Miller, M.L. (2013). Cell-selective labeling using amino acid precursors for proteomic studies of multicellular environments. Nat. Methods *10*, 768–773.

46. Perez-Riverol, Y., Bai, J., Bandla, C., García-Seisdedos, D., Hewapathirana, S., Kamatchinathan, S., Kundu, D.J., Prakash, A., Frericks-Zipper, A., Eisenacher, M., et al. (2022). The PRIDE database resources in 2022: A hub for mass spectrometry-based proteomics evidences. Nucleic Acids Res. *50*, D543–D552.

47. Post, H., Penning, R., Fitzpatrick, M.A., Garrigues, L.B., Wu, W., MacGillavry, H.D., Hoogenraad, C.C., Heck, A.J.R., and Altelaar, A.F.M. (2017). Robust, Sensitive, and Automated Phosphopeptide Enrichment Optimized for Low Sample Amounts Applied to Primary Hippocampal Neurons. J. Proteome Res. *16*, 728–737.

48. Raudvere, U., Kolberg, L., Kuzmin, I., Arak, T., Adler, P., Peterson, H., and Vilo, J. (2019). Profiler: A web server for functional enrichment analysis and conversions of gene lists (2019 update). Nucleic Acids Res. *47*, W191–W198.

49. Zhou, Y., Zhou, B., Pache, L., Chang, M., Khodabakhshi, A.H., Tanaseichuk, O., Benner, C., and Chanda, S.K. (2019). Metascape provides a biologist-oriented resource for the analysis of systems-level datasets. Nat. Commun. *10*, 1523.

STAR★METHODS

KEY RESOURCES TABLE

REAGENT or RESOURCE	SOURCE	IDENTIFIER
Antibodies		
Vinculin	Sigma-Aldrich	Cat#V9131; RRID:AB_477629)
Anti-Human CD3 Functional Grade Purified	Life Technologies	16-0037-85
Anti-Human CD28 Functional Grade Purified	Life Technologies	16-0289-85
Anti-Human CXCL10 PE	Biolegend	519504; RRID:AB_2561409
PD-L1/CD274-PECy7	BD Bioscience	558017; RRID:AB_396986
IFN-γ-APC	BD Bioscience	554702; RRID:AB_398580
Anti-human CD54 (ICAM-1) BV421	BD Bioscience	564077; RRID:AB_2738578
Anti-human Granzyme B AF700	BD pharmingen	560213
PD1-BV650	Biolegend	329739; RRID:AB_2629613
CD137-APC	BD Biosciences	550890; RRID:AB_398477
CD69-PE	Immunotools	21620694
CD25-PerCPCy5.5	Biolegend	302625; RRID:AB_2125479
TNFα-PE	Biolegend	502909; RRID:AB_315261
CD8-Pacific Blue	Biolegend	344717; RRID:AB_10551616
peroxidase conjugated anti-mouse IgG	Thermo Fisher	G-21040; RRID:AB_2536527
anti-rabbit IgG	Thermo Fisher	G-21234; RRID:AB_2536530
Granulins Polyclonal Antibody	ThermoFisher	PA5-27275; RRID:AB_2544751
Bacterial and virus strains		
E.coli strain:XL10-Gold Ultracompetent Cells	Internal stock	NA
1D3 virus	Internal stock	NA
Chemicals, peptides, and recombinant proteins		
proline	Sigma Aldrich	P5607
L-arginine:HCL 13C6, 99%; 15N4, 99%	Cambridge isotope laboratories	CNLM-539-H-0.25
L-lysine:2HCL 3,3,4,4,5,5,6,6-D8, 98%	Cambridge isotope laboratories	CNLM-539-H-0.25
Ficoll (1.078 g/mL)	FisherCientific	11,743,219
Retronectin	Takara	T100B
GolgiPlug™ Protein Transport Inhibitor	BD Biosciences	BD555029
LIVE/DEAD near IR marker	BD Biosciences	L34976
LIVE/DEAD Yellow marker	Themo Fisher	L3496
NVS-PAK1-1	MedChem	HY-100519
CFSE	Invitrogen	16-0289-85
phosphatase inhibitor, PhosSTOP	Roche	4906837001
protease inhibitor	Roche	11836170001
Lys C	Wako	NC9223464
10-plex TMT reagents	Thermo Fisher Scientific	LOT# UA275089
SepPak C18 cartridges	Waters	WAT036945
Critical commercial assays		
Dynabeads CD8 positive isolation kit	Invitrogen	11333D
BradfordProteinAssay	Bio-Rad	5,000,006
Super-Signal West Dura Extended Duration Substrate	ThemoFisher	34,075
Foxp3 Transcription Factor Staining Buffer kit	Invitrogen	00-5523-00
AssayMap BRAVO platform	Agilent Technologies	NA
C18 trapping column (PepMap100, 5um, 100A, 5mm x 300um)	Thermo Scientiifc	164946

(*Continued on next page*)

Continued

REAGENT or RESOURCE	SOURCE	IDENTIFIER
C18 analytical column (120 EC-C18, 2.7uM, 50 cm x 75um)	Agilent Poroshell	NA
Deposited data		
ProteomeXchange Consortium	This paper	PXD046734
Satpathy et al. phosphoproteome cohort	Satpathy et al.[28]	NA
Gillette et al. phosphoproteome cohort	Gillette et al.[29]	NA
Homo sapiens database	UniProt, 2017; 21,008 entries	NA
Experimental models: Cell lines		
LCLC-103H	Internal stock	RRID:CVCL_1375
A549	Internal stock	RRID:CVCL_0023
EBC-1	Internal stock	RRID:CVCL_2891
NCI-H358	Internal stock	RRID:CVCL_1559
NCI-H1975	Internal stock	RRID:CVCL_1511
NCI-H441	Internal stock	RRID:CVCL_1561
NCI-H460	Internal stock	RRID:CVCL_0459
NCI-H2122	Internal stock	RRID:CVCL_1531
D10	Internal stock	NA
A875	Internal stock	RRID:CVCL_4733
DU-145	Internal stock	RRID:CVCL_0105
SW-480	Internal stock	RRID:CVCL_0546
Software and algorithms		
GraphPadPrism9 (v9.0.0)	GraphpadSoftwareInc.	https://www.graphpad.com/scientific-software/prism/
R (v4.1.1	R	https://cran.r-project.org/
RStudio (v1.4.1106)	R Studio, PBC	https://www.rstudio.com/
Flowjo (v10.8.2)	Flowjo	https://www.flowjo.com/solutions/flowjo
MaxQuant software (v 2.0.1.0 and 1.6.10.43)	MaxQuant	https://www.maxquant.org/

RESOURCE AVAILABILITY

Lead contact

Information and requests for resources and reagents should be directed to the correspondent authors Daniel S. Peeper (d.peeper@nki.nl) and Maarten Altelaar (m.altelaar@nki.nl). Lead contact is Daniel S. Peeper (d.peeper@nki.nl).

Materials availability

The materials generated in this study did not generate unique new reagents.

Data and code availability

- Data are available within the article or its supplementary materials. All mass spectrometry proteomics data have been deposited to the ProteomeXchange Consortium via the PRIDE[46] partner repository with the dataset identifier PXD046734; (Dataset:PXD046734) . Protein and phosphopeptide abundances for tumor cells, T cells, and newly translated proteins can be found in Tables S1 and S2.
- This paper does not report original code.
- Any additional information required to reanalyze the data reported in this work paper is available from the lead contact upon request.

EXPERIMENTAL MODEL AND STUDY PARTICIPANT DETAILS

Cell culture

Tumor cell lines were obtained from the Peeper laboratory stock. They were cultured in RPMI (Thermofisher, 21875034) supplemented with 10% fetal bovine serum (Sigma, 3101120) and 100U/ml Penicillin-Streptomycin (Invitrogen, 15140-122). They were

transduced with the HLA-A*02:01-MART1-mPlum lentiviral plasmid.[18] They were tested for mycoplasma by PCR monthly. The following cell lines were used in this study: LCLC-103H (RRID:CVCL_1375), A549 (RRID:CVCL_0023), EBC-1 (RRID:CVCL_2891), NCI-H358 (RRID:CVCL_1559), NCI-H1975 (RRID:CVCL_1511), NCI-H441 (RRID:CVCL_1561), NCI-H460 (RRID:CVCL_0459), NCI-H2122 (RRID:CVCL_1531), D10, A875 (RRID:CVCL_4733), DU-145 (RRID:CVCL_0105) and SW-480 (RRID:CVCL_0546).

CD8 T cells were isolated with Dynabeads from PBMCs from healthy donors, activated with αCD3 and αCD28 antibodies (eBioscience, 5 μg per well) for 48h and transduced with a MART-1 specific TCR by spinfection.

METHOD DETAILS

SILAC labeling

Tumor cell lines were cultured in "Heavy" $^{8}K^{10}R$ medium consisting of RPMI 1640 Medium for SILAC (88365, Thermofisher) with 10% dialyzed fetal bovine serum (Fisher Scientific, 15605639), 100U/ml Penicillin-Streptomycin (Invitrogen, 15140-122), 0.04 mg/L proline (Sigma Aldrich, P5607), 100ug/ml L-arginine:HCL 13C6, 99%; 15N4, 99% (Cambridge isotope laboratories, CNLM-539-H-0.25) and 40 mg/ml L-lysine:2HCL 3,3,4,4,5,5,6,6-D8, 98% (Cambridge isotope laboratories, CNLM-539-H-0.25). Cells were grown in this medium for at least 5 doublings before testing isotope incorporation by MS.

T cell:tumor co-culture with SILAC

Stable-isotope labeled tumor cells were counted and seeded at $3x10^6$ cells per 10 cm Petri dish. The next day, $3x10^6$ MART-1-transduced T cells were added and incubated for the indicated hours (2, 4 or 6) in "Intermediate" $^{4}K^{6}R$ medium consisting of RPMI 1640 Medium for SILAC (88365, Thermofisher) with 10% dialyzed fetal bovine serum (15605639, Fisher Scientific), 100U/ml Penicillin-Streptomycin (Invitrogen, 15140-122), 0.04 mg/L proline (Sigma Aldrich, P5607), 100ug/ml L-arginine:HCL 13C6, 99% (Cambridge isotope laboratories, CLM-2265-H-0.1) and 40 mg/ml L-lysine:2HCL 4,4,5,5-D4, 96–98% (Cambridge isotope laboratories, DLM-2640). After co-culture, T cells were washed away, spun down at 1700 rpm for 5 min and washed with PBS. Tumor cells were washed 2x PBS, scrapped in 1 mL PBS and pelleted by spin down at 1500 rpm for 5 min and combined together with the corresponding T cell samples recovered from the media.

HySic mass spectrometry sample preparation

Cell pellets were resuspended in 300 μL of 1%(w/v) sodium deoxycholate (SDC) lysis buffer (100mM Tris pH 8.0, 10mM Tris (2-carboxyethyl) phosphine (TCEP), 40mM chloroacetamide, phosphatase inhibitor (PhosSTOP, Roche), and protease inhibitor (complete mini EDTA-free, Roche). Resuspended samples were boiled for 5 min at 95°C and sonicated for 15 min in the Bioruptor (Diagenode) at 30 s on, 30 s off cycles. Lysates were clarified by centrifugation (20,000 x g for 10 min) and protein concentration was determined using a Bradford protein assay. For each sample, 210 μg of protein was digested using Lys C (Wako) at an enzyme:protein ratio of 1:100 and trypsin (Sigma) at 1:50 ratio overnight at 37°C. Samples were acidified by addition of formic acid (FA) to a final concentration of 2% (v/v). Samples were centrifuged (20,000 x g for 10 min) and desalted using 5 μL C18 cartridges on the AssayMap BRAVO platform (Agilent Technologies). For each sample, 10 μg of digested protein was saved for proteome analysis and the remaining 200 μg of digested protein was enriched for phosphopeptides using 5 μL Fe(III)NTA cartridges on the AssayMap BRAVO platform.[47] Samples were dissolved in 200 μL loading buffer (80% acetonitrile (ACN)/0.1% TFA). Fe(III)-NTA 5 μL cartridges were primed with 200 μL of 0.1% TFA in ACN and equilibrated with 250 μL of loading buffer. Then, the column was loaded the samples at a loading speed of 5 μL/min. The columns were washed with 250 μL loading buffer and eluted with 35 μL of 5% ammonia solution into 35 μL of 10% FA. All elusions were dried in a vacuum centrifuge and resuspended in 2% FA for LC-MS injection. For phosphopeptide elutions, samples were injected twice when possible.

Generation of 'T0' control samples

For 'T0' samples, $^{8}K^{10}R$ labeled tumor cells were incubated for 4 h in $^{4}K^{6}R$ media, without T cells, to establish an internal control for background translation. Following cell lysis, tumor T0 samples were mixed with lysed T cells (labeled $^{0}K^{0}R$) to create an artificially mixed proteome sample. This mixed T0 sample possessed a comparable MS1 profile to 2h, 4h, and 6h co-culture lysates, which was necessary for subsequent LFQ analysis.

HySic mass spectrometry data acquisition

Proteome and phosphoproteome data were acquired on either an Orbitrap Exploris 480 MS (Thermo Scientific) coupled to an UltiMate 3000 UHPLC (Thermo Scientific) fitted with a C18 trapping column (PepMap100, 5um, 100A, 5mm x 300um; Thermo Scientiifc) and a homemade C18 analytical column (120 EC-C18, 2.7uM, 50 cm x 75um; Agilent Poroshell) or acquired on an Orbitrap Q Exactive H-FX MS (Thermo Scientific) coupled to an Agilent 1290 Infinity UHPLC system fitted with a Reprosil pur C18 trap column (100um x 2cm, 3um, Dr. Maisch) and a homemade C18 analytical column, described above. The different instrumentation used corresponds to the two separate experimental batches (HySic Study I: A549 and NCI-H358 cell lines, H-FX-Agilent 1290 setup; HySic study II: LCLC-103H and EBC-1 cell lines, Explores 480-UltiMate setup). The LC-MS parameters for each experiment were as follows: SI proteome data were collected over a 175 min run following 5 min of trapping with buffer A (0.1% FA). Peptides were eluted over a 155 min gradient from 10% to 44% solvent B (0.1%FA, 80%ACN) at a flow rate of 300 nL/min, followed by a wash and

re-equilibration step. MS data were acquired in Data-Dependent mode with MS1 settings at 60,000 resolution, scan-range 375-1600 m/z, AGC target at 3E6 and max ion injection time (IT) 20 msec. HCD-MS2 spectra were collected at 30,000 resolution for the top 15 precursors using an NCE of 27, max IT of 65 msec, AGC target of 1E5, isolation window of 1.4 Da, fixed first mass set at 120 m/z, and a dynamic exclusion time of 30 s. Study I phosphoproteome data were collected for 115 min using a 9%–36% solvent B elution gradient over 95min. MS settings were identical as above with the following adjustments: the top 12 precursors were selected for fragmentation with a max IT of 85 msec and dynamic exclusion of 18 s. Study II proteome and phosphoproteome data were collected using settings identical to Study I with the following exceptions: AGC targets were set to 'standard' and max IT was set to 'auto'. MS2 scans were collected for a fixed cycle window of 3 s with an NCE of 28 and a dynamic exclusion time of 24 s for proteome and 16 s for phosphoproteome data.

HySic mass spectrometry data processing

MS raw files were searched using MaxQuant software (versions 2.0.1.0 and 1.6.10.43) against a reviewed homo sapiens database (UniProt, 2017; 21,008 entries) and a contaminant database. Study I (A549 and NCI-H358 tumor cell lines) and Study II (LCLC-103H and EBC-1 tumor cell lines) raw files were processed separately, and in each case proteome and phosphoproteome data were searched separately, generating a total of 4 datasets. For each MaxQuant search, labeling multiplicity was set to 3 with Arg6, Lys4 and Arg10 and Lys8 selected for medium and heavy labels, respectively. Match-between-runs was enabled, Re-quantify was disabled, fixed modifications were set to carbamidomethylation, variable modifications were set to methionine oxidation and protein N-term acetylation, and all other MaxQuant parameters were set to default. For phosphoproteome searches, phosphorylation at STY residues was selected as an additional variable modification. Protein and phosphosite intensities were extracted from MaxQuant output files for each SILAC label independently ('H', 'M', 'L'). All SILAC ratio data were discarded. Extracted protein and peptide intensities were further processed in R using in-house scripts. Within each experimental dataset, the total summed intensity for each raw file were compared to identify sample outliers (i.e., failed sample injections). An outlier was defined as a sample with a signal intensity > 2x standard deviation below the mean of all samples. No outliers were identified in either proteome dataset, however, several injections were discarded from phosphoproteome data (Figure S1D). Next, to correct for differences in sample loading or instrument performance, samples were median normalized based on the combined intensities of all SILAC channels in each sample. Injection replicates were averaged to generate one dataset per biological replicate. After this step, SILAC intensities for each sample were processed independently, generating a total of 3 data tables for each experimental dataset: tumor cell, T cell, and Newly Synthesized proteins. Extracted T cell and tumor cell data were median normalized to correct for any differences in cell mixing across co-culture samples (Figure S1E). Newly Synthesized proteins did not undergo a second normalization because these abundances are not expected to be similar across all samples, but rather increase with time (Figure S1E). All data tables can be accessed in Table S1 (HySic Proteome) and Table S2 (HySic Phosphoproteome).

HySic mass spectrometry data filtering

All datasets were filtered to require at least 2 biological replicates (BR) in at least one experimental condition. Further filtration steps were applied per dataset as described below. Phosphoproteome data for tumor cells and T cells was filtered to required phosphosite quantification in at least 2/3 BRs for one or more co-culture incubation time points (2h, 4h, 6h). For heatmap analysis, phosphosite changes relative to time point zero (T0) were calculated to identify phosphorylation changed induced by co-culture conditions. Within each tumor cell line co-culture series, T0 values were averaged and phosphosite abundances were normalized to T0 averages. For T cell calculations, T0 values were averaged within experimental batches, as these T cells were aliquots from the same donor. For phosphosites with no T0 values in any BR, data were imputed using the minimum value from the dataset. T0 ratio data were median normalized and a one-way ANOVA test was performed to identify significantly changing phosphosites within each coculture treatment series (FDR <0.15, Benjamini-Hochberg p value correction). Phosphosites with no T0 values were also included in the 'significant hits' list as they may represent 'on/off' phosphorylation states. Finally, data were filtered for phosphosites that show significant changes within at least three of the four co-cultured cell lines for tumor cells and across both donors for T cells.

Proteome data for tumor and T cells was filtered to require measurements at T0 time points. For heatmap analysis, T0 ratios were calculated as described above, and data were filtered to require significant downregulation relative to T0 (FDR <0.15, Benjamini-Hochberg p value correction) in at least one cell line. Data were further filtered to include proteins that were decreasing in at least three of the four co-cultured cell lines at the 6h timepoints.

For newly synthesized proteins, proteome data were filtered to require quantification in at least 2/3 BR in the 4h and/or 6h co-culture time points. Proteins were further filtered to require either no measurement in T0 controls for background translation or have at least a 2-fold increase above background translation at 4h and 4-fold increase above background translation at 6hr. For newly synthesized phosphoproteome data, similar filtering steps were applied. For inclusion in heatmap analysis, phosphosites must also show quantification at 6h in at least three of the four co-cultured cell lines.

T cell PAK1 inhibitor MS sample preparation

T cell pellets were lysed in a 1% SDC buffer, quantified, digested (60 μg/sample), desalted, and dried as described above. Digested samples were resuspended in 80 μL of 50 mM HEPES buffer and labeled with 10-plex TMT reagents (Thermo Fisher Scientific, LOT# UA275089) at a label:protein ratio of 2:1 for 1.5 h, shaking at room temperature. To check labeling efficiency and mixing ratios, 2 μL of

each sample was combined in acidic solution for an LC-MS test run. After complete labeling was confirmed, samples were quenched using 6 μL of 5% hydroxylamine and incubate 15 min at room temperature. Labeled samples were next mixed equally and desalted using SepPak C18 cartridges (Waters). Alongside the individual samples, a pooled reference sample was generated from an aliquot of all digests. This pooled reference sample labeled was spiked into each TMT-10plex pool to act as a universal standard for data normalization. Following desalting, an aliquot of each TMT pool was reserved for proteome analysis and the rest was dried in the vacuum-centrifuge for phosphopeptide preparation. The workflow followed for the TMT sample preparation is outlined in (Figure S5A).

Before enrichment of phosphopeptides, the TMT labeled samples were fractionated using reversed-phase S cartridges and high pH buffer (200mM NH_4HCO_3, pH 10) on the AssayMap BRAVO Platform. Fractions were eluted with four steps of increasing buffer B (100% ACN): 22%, 30%, 36%, and 70% directly into 10% FA to neutralize the pH. Next, phosphopeptides were enriched for each fraction on the AssayMap BRAVO platform following the method described above.

T cell PAK1 inhibitor MS data acquisition

TMT labeled samples for proteome analysis were measured using an Orbitrap Fusion Lumos Tribrid MS (Thermo Scientific) coupled to an UltiMate 3000 UHPLC system (Thermo Scientific) fitted with a μ-precolumn (C18 PepMap100, 5 μm, 100 Å, 5 mm × 300 μm; Thermo Scientific), and a homemade analytical column (120 EC-C18, 2.4 μm, 50 cm × 75 μm; Agilent Poroshell). Samples were resuspended in 2% FA solution and loaded in solvent A (0.1% FA in water) with a flow rate of 30 μL/min and eluted using a 175 min gradient at a flow rate of 300 nL/min. The gradient for peptides was as follows: 9% solvent B (0.1% FA in 80% ACN) for 1 min, 9–13% B for 1 min, 13–40% B for 155 min, followed by a wash and re-equilibration step. The MS was operated in TMT-SPS-MS3 mode. The following MS settings were applied. For MS1 scans, detector type: Orbitrap; resolution: 60,000; scan range (m/z): 375–1500 Th; AGC target: standard; maximum injection time mode: auto; intensity threshold: 5 x10^3; charge state: 2–6; dynamic exclusion: 30 s. For MS2 scans, isolation mode: quadrupole; isolation windows (m/z): 1.2 Th; CID collision energy: 35%; precursor selection mass range (m/z): 400–1600 Th; precursor ion exclusion mass width: low 25 ppm, high 25 ppm; isobaric tag loss exclusion: TMT. For MS3 scans, number of SPS precursors: 5; MS isolation window (m/z): 1.3 Th; MS2 isolation window (m/z): 2 Th; activation type: HCD; collision energy: 65%; detector type: Orbitrap; resolution: 50,000; scan range: 100–500 Th; normalized AGC target: 200%; maximum injection time: 200 ms.

TMT labeled phosphopeptide samples were measured using MS2-based quantification on an Orbitrap Exploris 480 mass spectrometer (Thermo Fisher Scientific) coupled to an UltiMate 3000 UHPLC system (Thermo Fisher Scientific) as described above. Data were acquired using a 115 min acquisition method, as described above for the HySic phosphoproteome, with the following exceptions: MS2 resolution was set to 45,000, MS2 isolation window was reduced to 1.2, and NCE was increased to 32.

T cell PAK1 inhibitor MS data processing

Raw data files were processed with Proteome Discover 2.4 (Thermo Fisher Scientific) using Sequest HT and with a Swiss-Prot Homo sapiens database (version. 20220720) and a contaminant database. The isotopic impurities of the TMT reagent were corrected using the values specified by the manufacturer. The search parameters for proteomic data were as follows: enzyme was set to trypsin, with up to 2 missed cleavage sites. Fragment mass tolerance was set to 0.5 Da and precursor mass tolerance to 10 ppm. Carbamidomethyl of cysteine and TMT10-plex modification of lysine and peptides N terminus were set as static modifications. Oxidation of methionine and protein N-terminal acetylation were set as dynamic modifications. The reporter ions quantifier was set with HCD and MS3 (mass tolerance, 20 ppm). The PSM validation was performed using Percolator and the false discovery rate was set to 0.01. For the reporter ion quantification, unique + razor peptides were used. The threshold of co-isolation, average reporter S/N and SPS mass matches were 45, 10 and 65% respectively. The site probability threshold of peptide group modification was set 75. The FDR of peptide validator for PSMs and peptides were set to 1%. The FDR for protein FDR validator was also set to 1%. Minimum peptide length was set to 6 and minimum number of peptide sequence was set to 1 for peptide and protein filter. The parameters for phosphopeptide searches were as follows: Enzyme was set to trypsin, with up to 2 missed cleavage sites. Fragment mass tolerance was set to 0.06 Da and precursor mass tolerance to 20 ppm. Carbamidomethyl of cysteine and TMT10-plex modification of lysine and peptide N terminus were set as static modifications. Oxidation of methionine and protein N-terminal acetylation were set as dynamic modifications. Phosphorylation of serine, threonine and tyrosine was set as dynamic modifications. The reporter ions quantifier was set with HCD and MS2 (mass tolerance, 20 ppm). The PSM validation was performed with Percolator and the false discovery rate was set to 1%. For the reporter ion quantifier, unique + razor peptides were set for the quantification. The threshold of co-isolation, average reporter S/N and SPS mass matches were 45, 10 and 65% respectively. The site probability threshold of peptide group modification was set 75. The FDR of peptide validator for PSMs and peptides were set to 0.01. The FDR for protein FDR validator was also set to 0.01. Minimum peptide length was set to 6 and minimum number of peptide sequence was set to 1 for peptide and protein filter.

Flow cytometry

For flow cytometry analysis of T cell:tumor co-cultures, 5x10^4 tumor cells were co-cultured with 5×10^4 T cells (1:1 ratio) in a round bottom 96 well plate (Greiner, M9436-100EA) for 6 h. For intracellular staining, GolgiPlug Protein Transport Inhibitor (1:1000, BD Biosciences, BD555029) was added after 3h co-culture. The Foxp3 Transcription Factor Staining Buffer kit (Invitrogen, 00-5523-00) was used following manufacturer instructions. For cell surface staining, cells were washed and stained with antibodies in 0.1% BSA PBS buffer on ice for 30 min protected from light. After staining, cells were washed twice and analyzed using LSRFortessa (BD

Biosciences). Cells were gated on FSC and SSC followed by single cell gate on FSC-HH/FSC and SSC-H/SSC and a LIVE/DEAD near IR marker (1:1000, BD Biosciences, L34976). The following antibodies were used: CXCL-10-PE (1:50, Biolegend, 519504), PD-L1/CD274-PECy7 (1:50, BD Bioscience, 558017), IFN-γ-APC (1:100, BD, 554702) and ICAM-1-BV421 (1:100, BD Bioscience, 564077).

For flow analysis of T cells treated with NVS-PAK1-1 or DMSO, cell surface or intracellular staining was performed as described above and the following antibodies were used: LIVE/DEAD Yellow marker (1:1000, Themo Fisher, L3496), PD1-BV650 (1:100, Biolegend, 329739), CD137-APC (1:100, BD Biosciences, 550890), CD69-PE (1:100, Immunotools, 21620694), CD25-PerCPCy5.5 (1:100, Biolegend, 302625) TNFα-PE (1:100, Biolegend, 502909), IFN-γ-APC (1:100, BD Biosciences, 554702) and CD8-Pacific Blue (1:100, Biolegend, 344717).

Western blotting

For Western blot analysis of T cell:tumor co-cultures, cells were seeded in a 10 cm Petri dish. After co-culture T cells were collected from the supernatant and spun down at 1700 rpm for 5 min. Tumor cells were washed twice with PBS and spun down at 1500 rpm for 5 min. Cell pellets were then resuspended in RIPA lysis buffer supplemented with protease/phosphatase inhibitor cocktail (1:1000, Thermo Fisher, 78440) and lysed for 30 min on ice. Protein concentration was quantified using Bio-Rad protein assay (Bio-Rad, 500-0006). Samples were analyzed on NuPAGE Bis-Tris 4-12% polyacrylamide-SDS gels (Life technologies, NP0321BOX) in MES buffer (Invitrogen, B000202). They were subsequently transferred into nitrocellulose membranes using iBlot (Thermo Fisher). Membranes were blocked for 1 h with 4% milk in PBST (0.2% Tween 20 in PBS). Primary antibodies were incubated overnight at 4°C. The next day membranes were washed with PBST and incubated with the secondary antibodies for 1 h at RT. After final wash in PBST, membranes were developed with Super Signal West Dura Extended Duration Substrate (Thermo Fisher, 34075) in ChemiDoc (Bio-Rad). The following antibodies were used: Vinculin (1:1000, Cell Signaling, 4650), Granulins polyclonal (Thermofisher, PA5-27275), peroxidase conjugated anti-mouse IgG (1:5000, Thermo Fisher, G-21040) and anti-rabbit IgG (1:5000, Thermo Fisher, G-21234).

PAK1 inhibitor treatment

For NVS-PAK1-1 (MedChem, HY-100519) treatment in co-culture experiments, 1-4x10^4 tumor cells were seeded in flat bottom 96 well plates (Greiner, 655180) with the indicated ratios of T cells. NVS-PAK1-1 was added at the indicated concentrations. Cell viability was determined using the Incucyte Zoom (HERACELL 240i incubator, Essen Bioscience) every 2 h by counting red fluorescence cells (mPlum expression of tumor cells). Cell count was normalized by subtraction of the cells counted at time 0h.

For NVS-PAK1-1 treatment of T cells, cells were re-activated in a non-culture treated 24 well plate that was coated with αCD3 and αCD28 (1:200 in PBS, Invitrogen, 16-0037-85) and αCD28 (1:200 in PBS, Invitrogen, 16-0289-85) for 24 h. Cells were then stained with CFSE (1:6000 in PBS, Biolegend, 423801) for 20 min at 37°C and washed with 2% BSA in FBS. T cells were then maintained at 10^6 cells/ml with NVS-PAK1-1 or DMSO for the indicated times. Cell surface markers were analyzed by flow cytometry as described above.

Bioinformatic analysis

For pathway enrichment analysis g:Profiler[48] and Metascape[49] were used. Reactome, Wikipathways, KEGG, Hallmark and GO significant ($p < 0.05$) pathways were shown when indicated.

QUANTIFICATION AND STATISTICAL ANALYSIS

All experimental data were tested for normal distribution with Saphiro-Wilk test. Datasets that passed normality were analyzed with parametric tests and datasets that did not pass were analyzed with non-parametric. In each figure legend the statistical test is indicated. Data were analyzed and plotted in Graphpad Prism and R.

Cell Reports, Volume *43*

Supplemental information

Phosphoprotein dynamics of interacting T cells and tumor cells by HySic

Sofía Ibáñez-Molero, Joannes T.M. Pruijs, Alisha Atmopawiro, Fujia Wang, Alexandra M. Terry, Maarten Altelaar, Daniel S. Peeper, and Kelly E. Stecker

S. 1

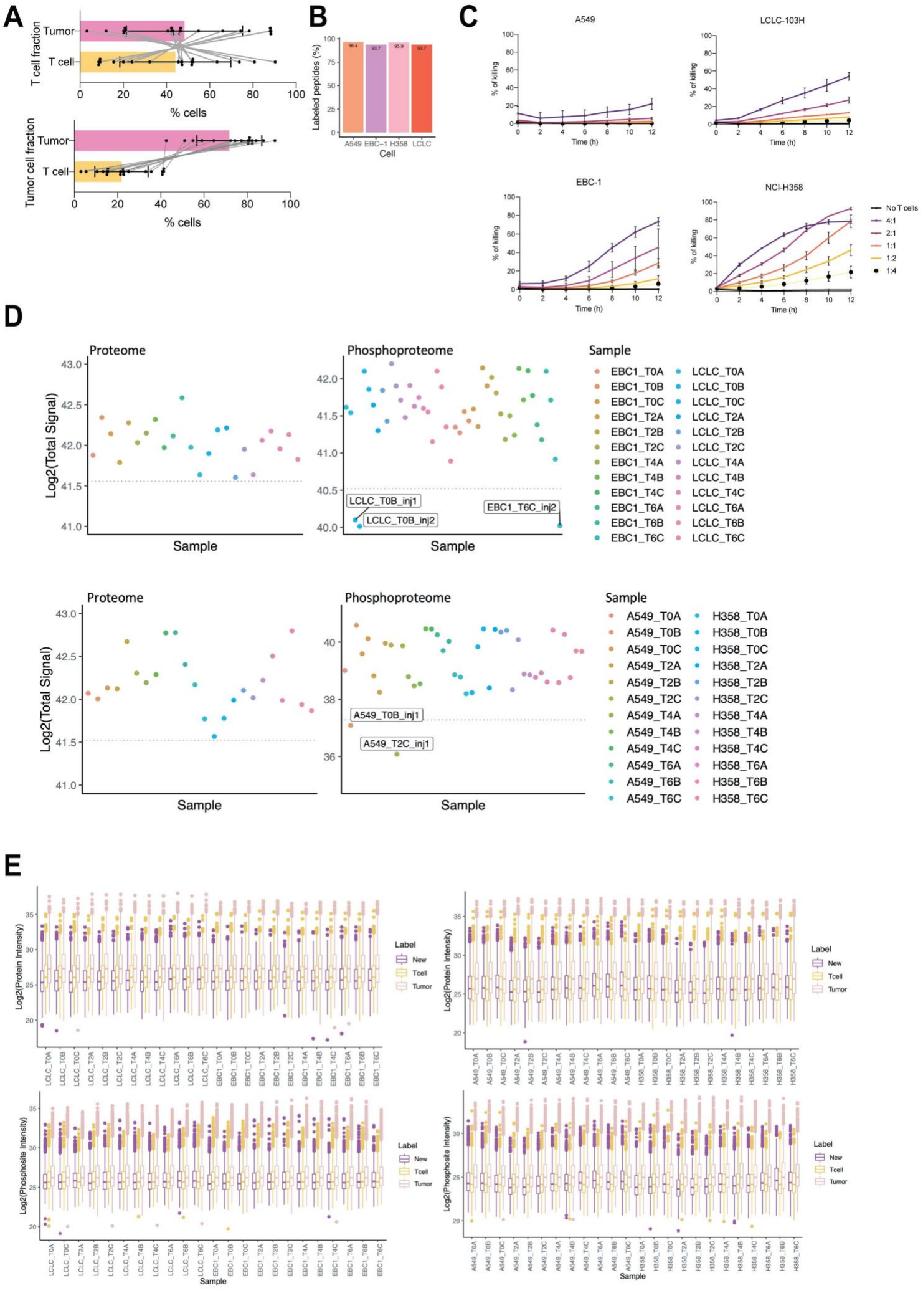
A
Tumor
T cell
T cell fraction
% cells
Tumor cell fraction
B
Labeled peptides (%)
A549 EBC−1 H358 LCLC
Cell
C
A549
LCLC-103H
EBC-1
NCI-H358
% of killing
Time (h)
No T cells
4:1
2:1
1:1
1:2
1:4
D
Proteome
Phosphoproteome
Log2(Total Signal)
Sample
LCLC_T0B_inj1
LCLC_T0B_inj2
EBC1_T6C_inj2
EBC1_T0A
EBC1_T0B
EBC1_T0C
EBC1_T2A
EBC1_T2B
EBC1_T2C
EBC1_T4A
EBC1_T4B
EBC1_T4C
EBC1_T6A
EBC1_T6B
EBC1_T6C
LCLC_T0A
LCLC_T0B
LCLC_T0C
LCLC_T2A
LCLC_T2B
LCLC_T2C
LCLC_T4A
LCLC_T4B
LCLC_T4C
LCLC_T6A
LCLC_T6B
LCLC_T6C
A549_T0B_inj1
A549_T2C_inj1
A549_T0A
A549_T0B
A549_T0C
A549_T2A
A549_T2B
A549_T2C
A549_T4A
A549_T4B
A549_T4C
A549_T6A
A549_T6B
A549_T6C
H358_T0A
H358_T0B
H358_T0C
H358_T2A
H358_T2B
H358_T2C
H358_T4A
H358_T4B
H358_T4C
H358_T6A
H358_T6B
H358_T6C
E
Log2(Protein Intensity)
Log2(Phosphosite Intensity)
Label
New
Tcell
Tumor
Sample

S. 2

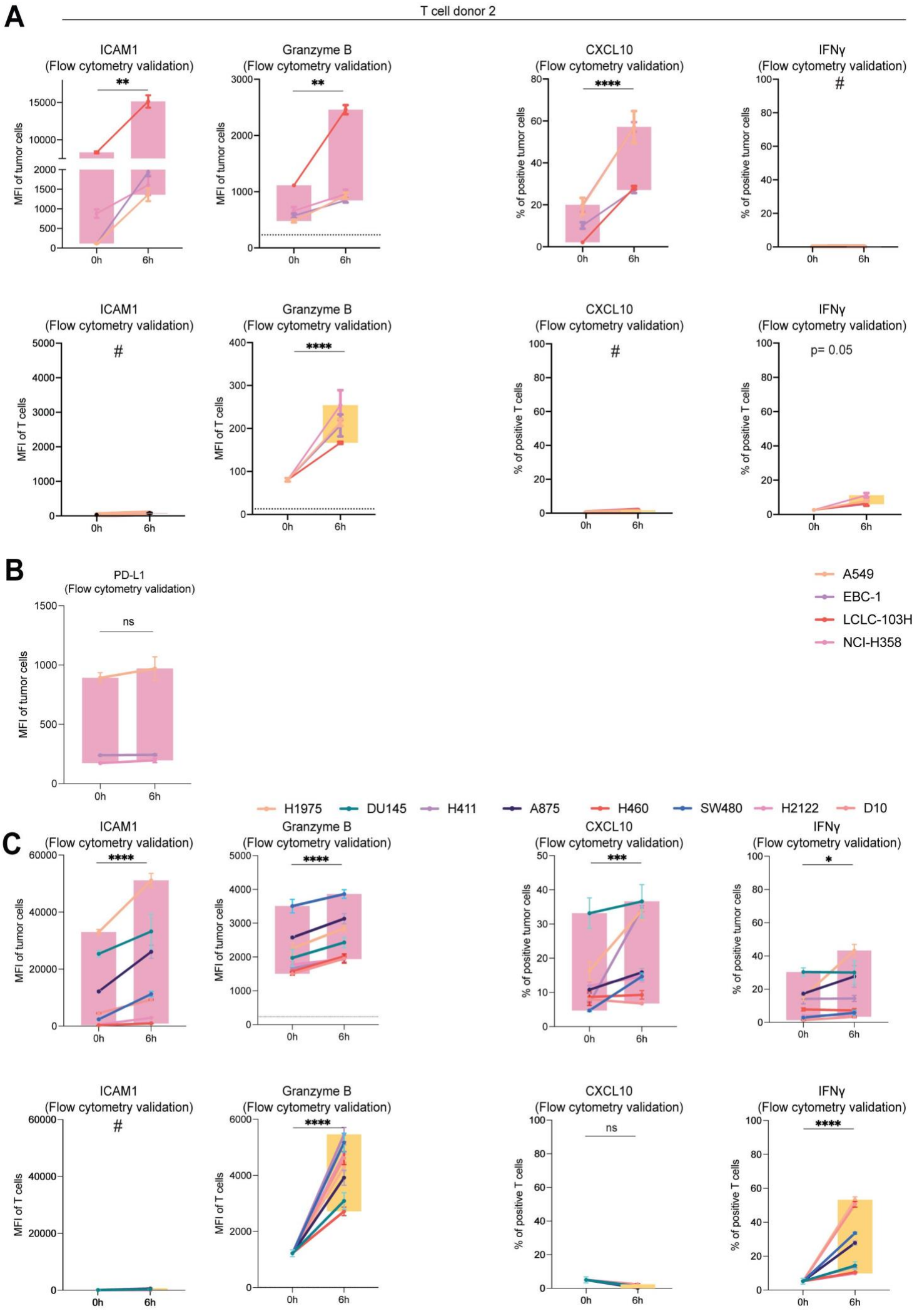
A
T cell donor 2
ICAM1
(Flow cytometry validation)
MFI of tumor cells
Granzyme B
(Flow cytometry validation)
MFI of tumor cells
CXCL10
(Flow cytometry validation)
% of positive tumor cells
IFNγ
(Flow cytometry validation)
% of positive tumor cells
ICAM1
(Flow cytometry validation)
MFI of T cells
Granzyme B
(Flow cytometry validation)
MFI of T cells
CXCL10
(Flow cytometry validation)
% of positive T cells
IFNγ
(Flow cytometry validation)
p= 0.05
% of positive T cells
0h
6h
B
PD-L1
(Flow cytometry validation)
ns
MFI of tumor cells
A549
EBC-1
LCLC-103H
NCI-H358
H1975
DU145
H411
A875
H460
SW480
H2122
D10
C
ICAM1
(Flow cytometry validation)
Granzyme B
(Flow cytometry validation)
CXCL10
(Flow cytometry validation)
IFNγ
(Flow cytometry validation)
MFI of tumor cells
% of positive tumor cells
MFI of T cells
% of positive T cells
ns
p= 0.05

S. 3

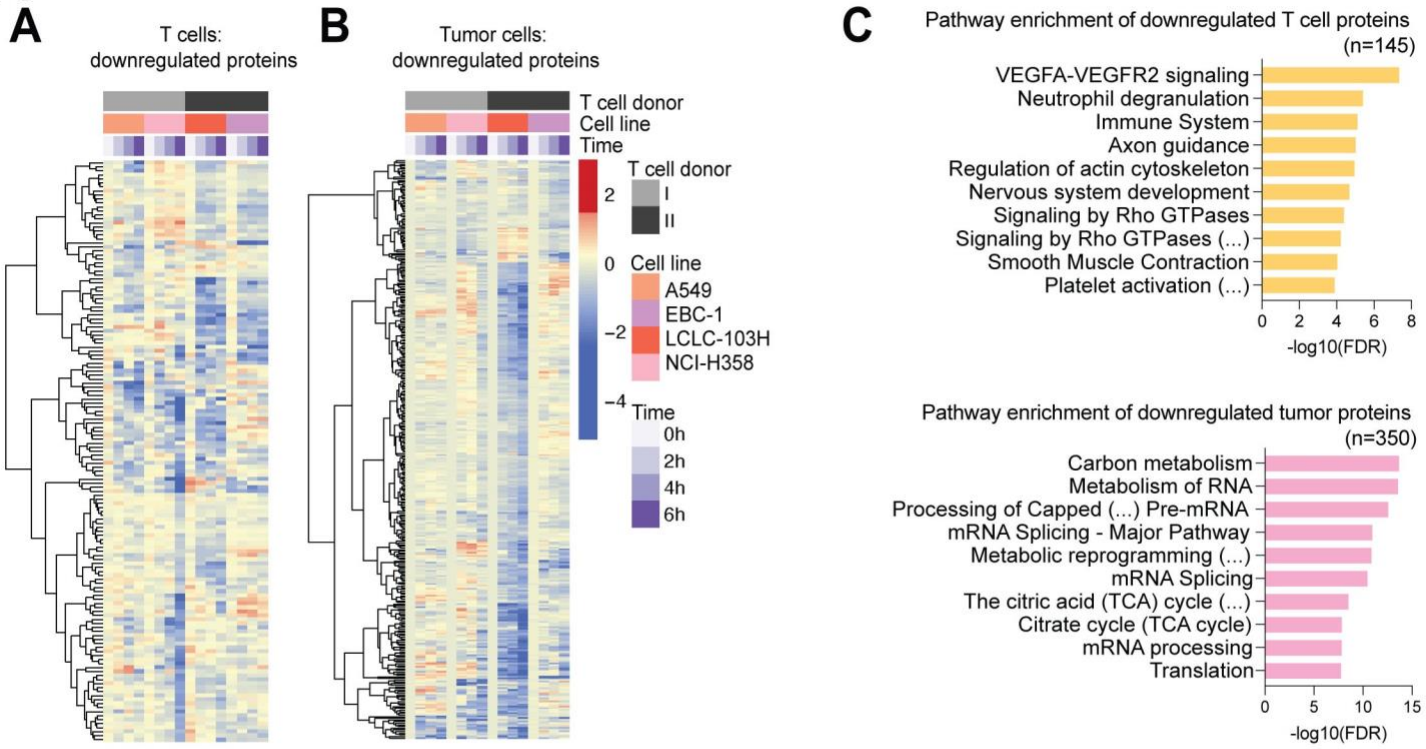
A
T cells:
downregulated proteins
B
Tumor cells:
downregulated proteins
T cell donor
Cell line
Time
T cell donor
I
II
Cell line
A549
EBC-1
LCLC-103H
NCI-H358
Time
0h
2h
4h
6h
2
0
−2
−4
C
Pathway enrichment of downregulated T cell proteins
(n=145)
VEGFA-VEGFR2 signaling
Neutrophil degranulation
Immune System
Axon guidance
Regulation of actin cytoskeleton
Nervous system development
Signaling by Rho GTPases
Signaling by Rho GTPases (...)
Smooth Muscle Contraction
Platelet activation (...)
0 2 4 6 8
-log10(FDR)
Pathway enrichment of downregulated tumor proteins
(n=350)
Carbon metabolism
Metabolism of RNA
Processing of Capped (...) Pre-mRNA
mRNA Splicing - Major Pathway
Metabolic reprogramming (...)
mRNA Splicing
The citric acid (TCA) cycle (...)
Citrate cycle (TCA cycle)
mRNA processing
Translation
0 5 10 15
-log10(FDR)

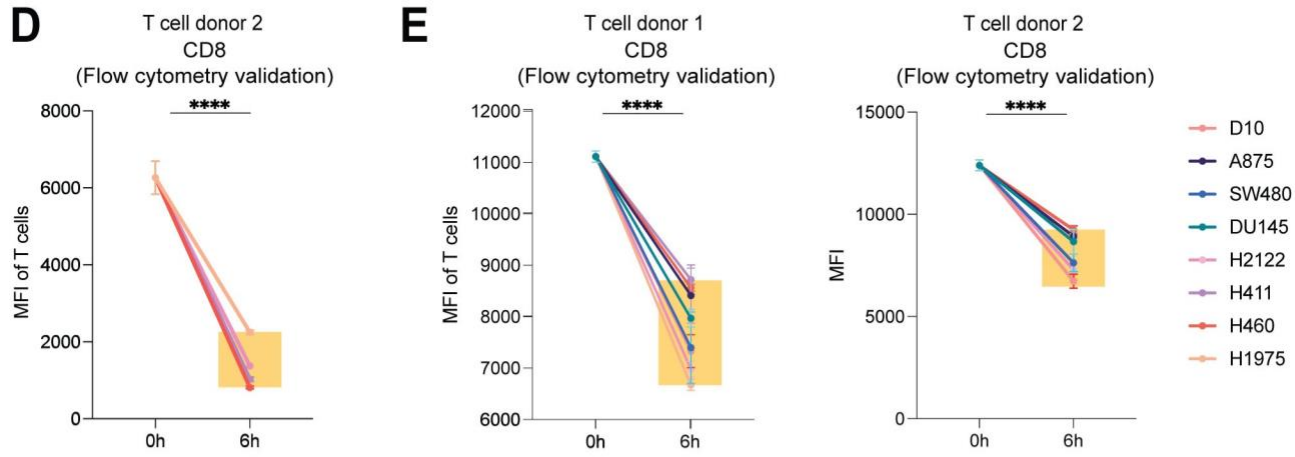
D
T cell donor 2
CD8
(Flow cytometry validation)
****
MFI of T cells
8000
6000
4000
2000
0
0h
6h
E
T cell donor 1
CD8
(Flow cytometry validation)
****
MFI of T cells
12000
11000
10000
9000
8000
7000
6000
0h
6h
T cell donor 2
CD8
(Flow cytometry validation)
****
MFI
15000
10000
5000
0
0h
6h
D10
A875
SW480
DU145
H2122
H411
H460
H1975

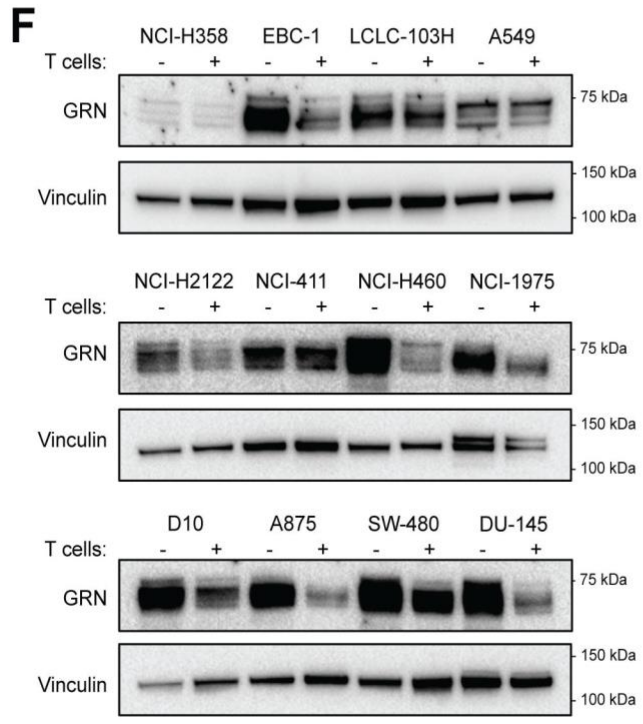
F
NCI-H358
EBC-1
LCLC-103H
A549
T cells:
- + - + - + - +
GRN
75 kDa
Vinculin
150 kDa
100 kDa
NCI-H2122
NCI-411
NCI-H460
NCI-1975
T cells:
- + - + - + - +
GRN
75 kDa
Vinculin
150 kDa
100 kDa
D10
A875
SW-480
DU-145
T cells:
- + - + - + - +
GRN
75 kDa
Vinculin
150 kDa
100 kDa

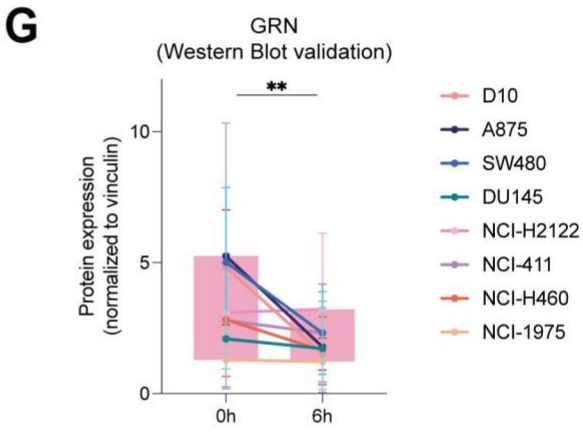
G
GRN
(Western Blot validation)
**
Protein expression
(normalized to vinculin)
10
5
0
0h
6h
D10
A875
SW480
DU145
NCI-H2122
NCI-411
NCI-H460
NCI-1975

S. 4

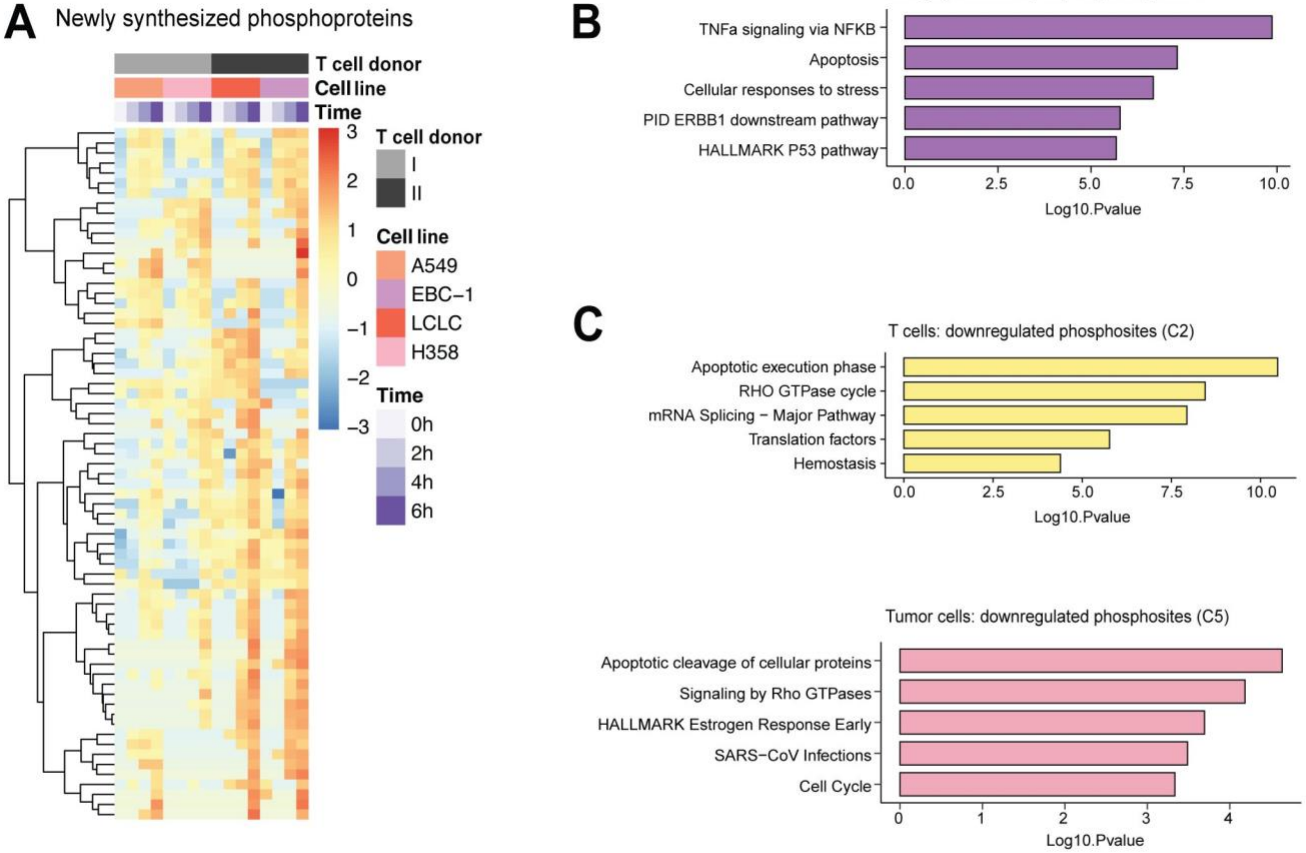
A
Newly synthesized phosphoproteins
T cell donor
Cell line
Time
T cell donor
I
II
Cell line
A549
EBC−1
LCLC
H358
Time
0h
2h
4h
6h
B
Newly synthesized phosphorylated proteins
TNFa signaling via NFKB
Apoptosis
Cellular responses to stress
PID ERBB1 downstream pathway
HALLMARK P53 pathway
Log10.Pvalue
C
T cells: downregulated phosphosites (C2)
Apoptotic execution phase
RHO GTPase cycle
mRNA Splicing − Major Pathway
Translation factors
Hemostasis
Log10.Pvalue
Tumor cells: downregulated phosphosites (C5)
Apoptotic cleavage of cellular proteins
Signaling by Rho GTPases
HALLMARK Estrogen Response Early
SARS−CoV Infections
Cell Cycle
Log10.Pvalue

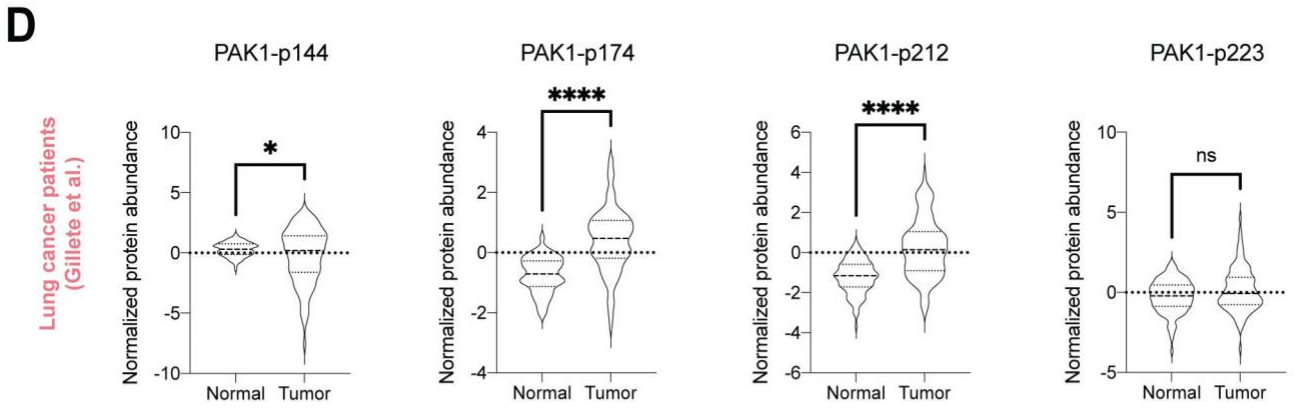
D
PAK1-p144
PAK1-p174
PAK1-p212
PAK1-p223
Lung cancer patients (Gillete et al.)
Normalized protein abundance
Normal
Tumor
*
****
****
ns

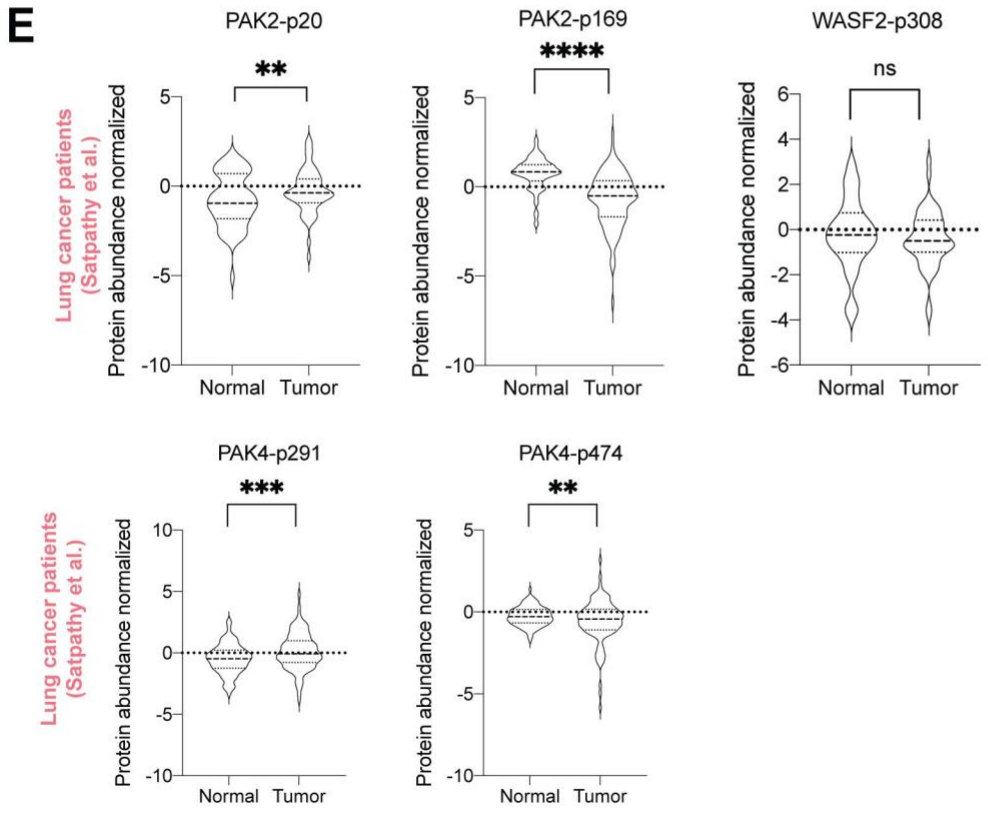
E
PAK2-p20
PAK2-p169
WASF2-p308
PAK4-p291
PAK4-p474
Lung cancer patients (Satpathy et al.)
Protein abundance normalized
Normal
Tumor
**
****
ns
***
**

S. 5

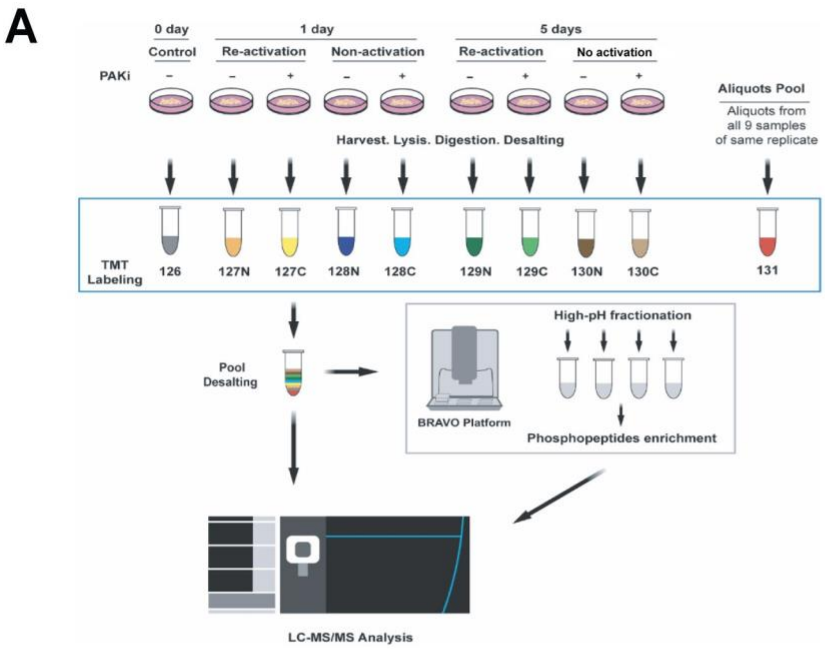
A
0 day
1 day
5 days
Control
Re-activation
Non-activation
Re-activation
No activation
PAKi
Aliquots Pool
Aliquots from all 9 samples of same replicate
Harvest. Lysis. Digestion. Desalting
TMT Labeling
126
127N
127C
128N
128C
129N
129C
130N
130C
131
Pool Desalting
High-pH fractionation
BRAVO Platform
Phosphopeptides enrichment
LC-MS/MS Analysis

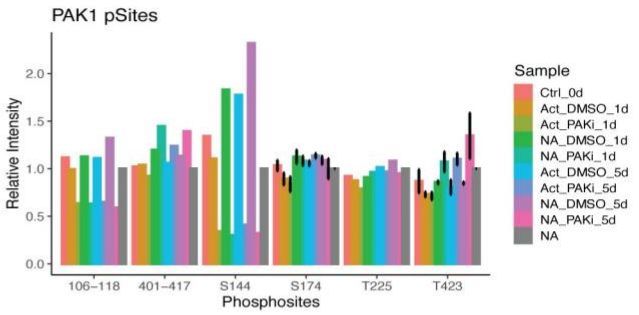
B
PAK1 pSites
Relative Intensity
Phosphosites
106–118
401–417
S144
S174
T225
T423
Sample
Ctrl_0d
Act_DMSO_1d
Act_PAKi_1d
NA_DMSO_1d
NA_PAKi_1d
Act_DMSO_5d
Act_PAKi_5d
NA_DMSO_5d
NA_PAKi_5d
NA

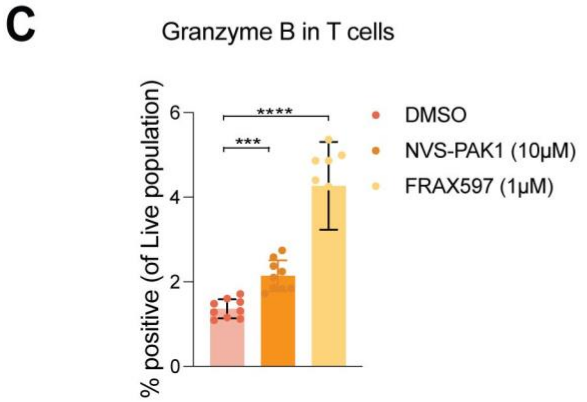
C
Granzyme B in T cells
% positive (of Live population)
****
***
DMSO
NVS-PAK1 (10μM)
FRAX597 (1μM)

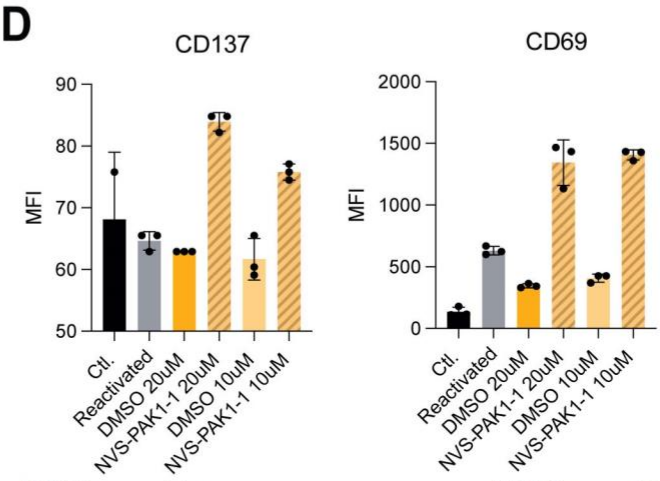
D
CD137
CD69
MFI
Ctl.
Reactivated
DMSO 20uM
NVS-PAK1-1 20uM
DMSO 10uM
NVS-PAK1-1 10uM

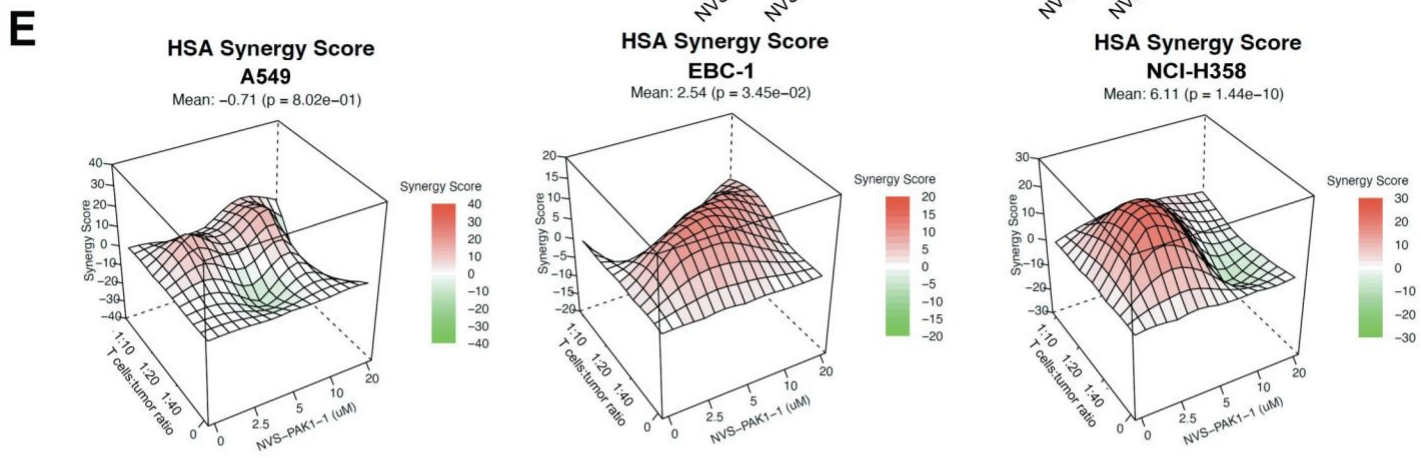
E
HSA Synergy Score
A549
Mean: −0.71 (p = 8.02e−01)
EBC-1
Mean: 2.54 (p = 3.45e−02)
NCI-H358
Mean: 6.11 (p = 1.44e−10)
Synergy Score
T cells:tumor ratio
NVS-PAK1-1 (uM)

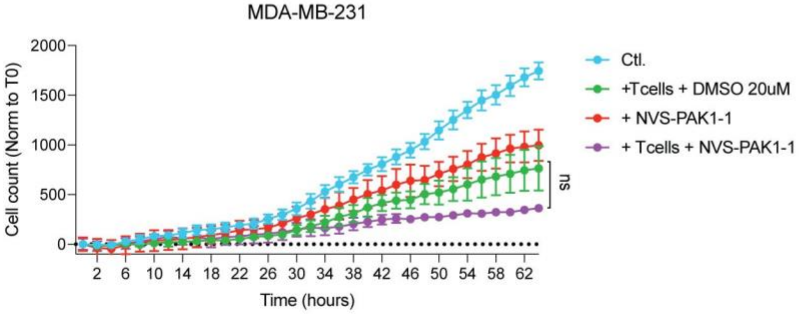
F
MDA-MB-231
Cell count (Norm to T0)
Time (hours)
Ctl.
+Tcells + DMSO 20uM
+ NVS-PAK1-1
+ Tcells + NVS-PAK1-1
ns

SUPPLEMENTAL FIGURE LEGENDS

Fig. S. 1. HySic set up, related to Figure 1. Supporting data for tumor:T cell co-culture system and HySic proteome and phosphoproteome dataset quality.

A) Percentage of cells measured by flow cytometry after co-culture in T cell (top) or tumor cell (bottom) fractions. Tumor cell percentage is represented in pink bar, T cell percentage is represented in yellow bar. Each dot represents a cell line. Grey lines connect the percentage of each cell types in individual cell lines.
B) SILAC labeling efficiency check. Bars represent heavy labeled peptide incorporation in each tumor cell line. Tumor cell lysates were analyzed by LC-MS and data was searched with K8 and R10 as a variable modification. Labeled and unlabeled peptides were counted. LCLC is abbreviation of LCLC-103H, H358 is abbreviation of NCI-H358.
C) Cytotoxic assay of tumor and T cells co-cultured in Incucyte® at the indicated ratios and timepoints. Viability of tumor cells was measured by green fluorescence counts (caspase3/7) every 2 hours. Percentage of killing calculated by normalization to the maximum killing reached at end point. Error bars represent SD of 3 technical replicates.
D) Sample outlier detection. Y axis represents log2 summed abundance for each sample. Dotted line represents 2x standard deviation from the mean of the entire dataset. Samples below the line were removed from the study. Phosphoproteome samples had two replicate injections on the MS. LCLC is abbreviation of LCLC-103H, H358 is abbreviation of NCI-H358.
E) Normalized protein and phosphosite expression levels. Y axis represents median log2 abundance for each sample. Tumor and T cell samples were normalized across all samples in the batch. Phosphoproteome injection replicates are averaged into generate one sample per biological replicate. LCLC is abbreviation of LCLC-103H, H358 is abbreviation of NCIH358.

Fig. S. 2 Validation of protein translation, related to figure 2. Flow cytometry validation of newly translated proteins identified by HySic.

A) Independent T cell donor experiment of Fig. 2E. Flow cytometry protein expression of the indicated proteins in either tumor cells (pink boxplots) or T cells (yellow boxplots). Each

cell line is represented by a colored dot with SD bars. Boxplot indicates deviation of four cell lines combined. **p-value<0.01, ****p-value<0.0001. 2-way ANOVA test used for statistical analysis. # indicates measurement below detection levels.

B) Flow cytometry expression of PD-L1 protein in tumor cells across three independent cell lines. ns indicates not significant.

C) Mean fluorescence intensity (MFI) or percentage of positive cells measured by flow cytometry of the indicated proteins in either tumor cells (pink boxplots) or T cells (yellow boxplots) before and after 6h co-culture. Each cell line is represented by a colored dot with SD bars. Boxplots indicate deviation of four cell lines combined. *p-value<0.01**pvalue<0.05, ***p-value<0.001, ****p-value<0.0001, ns=not significant. 2-way ANOVA test used for statistical analysis. # indicates below detection levels.

Fig. S. 3 Protein downregulation, related to figure 3. HySic quantification and validation of downregulated proteins in tumor cells and T cells.

A) Heatmap of significantly downregulated T cells proteins (FDR< 0.15) relative to T0 in at any co-culture timepoint in both T cell donors. FDR significance was determined by BenjaminiHochberg correction of unpaired t-test p-values. Proteins included in the heatmap were required to show a decreasing trend in at least 3/4 cell line co-cultures. Values represent log2 T0 normalized data. Heatmap contains 350 proteins.

B) Heatmap of significantly downregulated tumor cell proteins (FDR< 0.15) relative to T0 at any co-culture timepoint in at least one co-cultured cell line. FDR significance was determined by Benjamini-Hochberg correction of unpaired t-test p-values. Proteins included in the heatmap were required to show a decreasing trend in at least 3/4 cell lines. Values represent log2 T0 normalized data. Heatmap contains 145 proteins.

C) Top 10 enriched pathway in downregulated proteins detected in T cell (top) or tumor (bottom) channel. Enrichment was performed using *Gprofiler* with Reactome and WikiPathways databases. Downregulated proteins were selected from heatmap data in A & B. Pathways are listed from smallest to largest *p*-value.

D) Independent T cell donor experiment of Fig. 3C. Median fluorescence intensity (MFI) measured by flow cytometry of CD8 protein in T cells (yellow boxplots). Each cell line is

represented by a colored dot with SD bars. Boxplot indicates deviation of four cell lines combined. ***p-value<0.001, ****p-value<0.0001. 2-way ANOVA test used for statistical analysis.

E) MFI measured by flow cytometry of CD8 protein in T cells (yellow boxplots). Each cell line is represented by a colored dot with SD bars. Boxplot indicates deviation of four cell lines combined. ***p-value<0.001, ****p-value<0.0001. 2-way ANOVA test used for statistical analysis.

F) Measurement of Granulin and Vinculin protein expression by western blotting in the indicated tumor cell lines after 6h of co-culture with (+) or without (-) T cells.

G) Quantification of F normalized to vinculin. Each cell line is represented by a colored dot with SD bars. Boxplot indicates deviation of four cell lines combined. **p-value<0.05. 2way ANOVA test used for statistical analysis.

Fig. S. 4 Phosphorylation of newly synthesized proteins and patient phosphorylation PAK1 data, related to figure 4 and 5. Enrichment analysis of newly synthesized protein phosphorylation measured by HySic and PAK1 phosphorylation data from patient cohorts.

A) Heat map of 70 upregulated phosphosites in newly synthesized proteins in at least 3/4 co-cultured cell lines. Missing values were replaced with minimum value for heatmap visualization. Values represent log2 scaled abundances.

B) Pathway enrichment (Metascape) for 57 upregulated phosphorylated proteins from newly synthesized phosphosite heatmap. Top five enrichment terms are displayed.

C) Pathway enrichment (Metascape) for downregulated phosphorylated proteins from T cells (yellow, top; Heatmap Cluster 2; 121 unique phosphorylated proteins) and tumor cells (pink, bottom; Heatmap Cluster 5; 44 unique phosphorylated proteins) phosphosite heatmap. Top five enrichment terms are displayed.

D) Normalized phosphosite abundance from Satpathy *et a*l. of the indicated proteins in normal versus tumor tissue. Violin plots represent average of individual patient expression levels. *p<0,05, **p<0,01

E) Normalized phosphosites abundance from Gillete *et al*. of the indicated protein sites in normal versus tumor tissue. Violin plots represent average of individual patient expression levels. *p<0,05, **p<0,01

Fig. S. 5 PAK1 treatment in T cells, related to figure 5. Experimental setup for proteome and phosphoproteome analysis of PAK1i treated T cells and extended data analysis of PAKi treated T cells and tumor:T cell co-cultures.

A) Experimental workflow for TMT labeling and sample handling for PAK1 inhibitor treated T cells.

B) Phosphoproteomic analysis of T cells treated with DMSO or NVS-PAK1(10uM) for 1 or 5 days. T cells were activated (ACT) or not (NA). The relative intensities of the indicated PAK1 phosphosites are shown. Error bars represent standard deviation from 3 biological replicates.

C) Independent T cell donor experiment of Fig. 5B. Percentage of Granzyme B-positive T cells (of live population) upon NVS-PAK1 (10uM), FRAX587 (1uM) or DMSO treatment for 5 days. ***p-value<0.001, ****p-value<0.0001. 2-way ANOVA test used for statistical analysis.

D) Measure of protein expression by median fluorescence intensity (MFI) of CD137 or CD69 surface markers in flow cytometry of T cells treated with NVS-PAK1 (10uM or 20uM) or DMSO for 5 days. Error bars represent standard deviation from 3 technical replicates.

E) Synergy score (HSA) calculated with *Synergyfinder* on the indicated T cell:tumor cell ratios and drug concentrations for A549, EBC-1 and NCI-H358 cell lines. Score indicates the percentage of additive effect of using a combination of two treatments compare to the single agent.

F) Cytotoxic assay of tumor cells and T cells co-cultured with or without NVS-PAK1 in Incucyte®. Inhibitor concentration and T cell:tumor cell ratio was optimized per cell line; MDA-231 (10uM, 1:40). Data was normalized to 0h. Error bars represent SD of 3 technical replicates. Statistical analysis was performed by Friedman test. ns indicate not significant.